DISCUSSION

As ONB is a rare tumor, and to our knowledge no consensus exists regarding treatment, particularly for advanced cases. Review of the literature suggests that ONB is a surgical disease; the advent of craniofacial resection has clearly improved disease-free survival[6,15] and many authors recommend surgery as the initial treatment.[8,12,31,32] To improve locoregional control and survival, several authors recommend surgery followed by adjuvant radiotherapy.[10,12,31–33] Together, these reports suggest that the optimal treatment for surgically resectable cases is surgery followed by adjuvant radiotherapy.

Of our 12 patients with ONB, 5 had recurrent disease, 3 had intracranial invasion, 1 each had cervical lymph node metastases and distant metastases, and 2 were staged as Kadish B. Because these Kadish stage B patients declined surgery, treatment was initiated with chemotherapy and, if the disease was locoregional, continued with definitive radiotherapy after chemotherapy with ID.

Many authors have commented on the effectiveness of chemotherapy in the treatment of ONB.[7,12,14,18,19,34–37] Notwithstanding that these previous reports were based on single-institution experience with relatively small sample sizes, platinum-based chemotherapy was well regarded and considered effective.[14,36,37] We previously reported that 2 of 8 ONB patients responded to chemotherapy with mainly platinum-based regimens.[23] In our present analysis in 12 patients treated with ID, the response was also 25% (3 of 12 patients), but toxicities were mild and manageable. The median survival in the setting of recurrent or metastatic disease was approximately 12 months in previous reports,[22,31] but was 16.1 months in the current study. Although our sample size was small (n = 6), this result might indicate that chemotherapy for recurrent or metastatic ONB contributes to improving survival.

On univariate analysis, response rates to ID were significantly higher in patients aged <50 years and those with intracranial invasion. Rates for high-grade (Hyams grade III/IV) and low-grade (Hyams grade I/II) ONB were 37.5% (3 of 8 patients) and 0% (0 of 2 patients), respectively, but this difference was not statistically significant. Several authors have reported that the pathologic features of ONB correlate with its prognosis and response to chemotherapy,[1,10,18,26–28] whereas McElroy et al.[18] suggested that high-grade ONB (Hyams grade III/IV) may be sensitive to chemotherapy. Data from the current study may also suggest that ONB in younger patients and in those with aggressive disease extension may be sensitive to chemotherapy. The question of which subset of ONB patients will respond to chemotherapy is important but remains to be answered. The ability to predict response will allow the identification of those patients who should receive chemotherapy before definitive radiotherapy. Our present and previous reports may suggest that younger patients, those with aggressive disease extension, and those with high-grade histology (Hyams grade III/IV) may be sensitive to chemotherapy.[1,10,18,26–28] ONB is a rare disease, and identification of the clinical determinants of a response to chemotherapy will require the further accumulation of patients.

Although craniofacial resection is effective in controlling ONB, it is not without substantial risk and morbidity. Levine et al.[38] reported that of 27 patients undergoing this treatment, 20% experienced cerebrospinal fluid leakage and 12% had symptomatic postoperative pneumocephalus. Similarly, Richtsmeier et al.[39] reported 1 death and 9 major intracranial complications among a total of 26 patients. Radiotherapy as the initial treatment has been proposed as 1 means of obviating these complications. Elkon et al.[2] found that radiotherapy and surgery provided equivalent results in patients with early-stage disease. Similarly, a review from the Mayo Clinic indicated no significant difference in survival between patients receiving either radiotherapy or surgery alone.[10] However, recurrence with radiotherapy alone was approximately 60%.[2,33] Bhattacharyya et al.[13] reported excellent results in 9 cases of esthesioneuroblastoma (olfactory neuroblastoma) or neuroendocrine carcinoma treated using induction chemotherapy with cisplatin and etoposide followed by proton radiotherapy, with 8 of 9 patients exhibiting a dramatic response to therapy and remission of their tumor, which obviated the need for resection. Fitzek et al.[14] also reported promising results with the combination of induction chemotherapy and proton-photon radiotherapy for patients with advanced ONB. Nineteen patients with a sinonasal tumor (10 olfactory neuroblastoma and 9 neuroendocrine carcinoma) received chemotherapy with 2 courses of cisplatin and etoposide, followed by high-dose proton-photon radiotherapy to 69.2 GyE. Thirteen of the 19 responded to chemotherapy, with a 5-year survival rate of 74% and 5-year local control rate from the time of initial treatment of 88%. These findings demonstrated the possibility of nonsurgical treatment for ONB.

Nevertheless, radiotherapy for ONB is challenging because of the surrounding critical organs, including the optic pathway, brain, and brainstem. Thanks to its physical characteristics, proton radiotherapy provides better dose distribution than

photon radiotherapy, and is deemed a feasible and effective treatment modality for curative high-dose irradiation to the tumor volume without any increase in normal tissue toxicity.[24] We therefore used proton radiotherapy in cases in which the potential for damage to surrounding critical organs with photon radiotherapy could not be ruled out. To facilitate prevention to surrounding critical organs, we adopted induction chemotherapy with ID for locoregional ONB. Thus, ID was followed by photon radiation therapy of 66 Gy in 2-Gy fractions in 1 of 7 locoregional ONB patients and by proton radiotherapy of 65 GyE in 2.5-GyE fractions in 6 patients. The patient receiving photon radiation achieved a CR, as did 4 of the 6 patients receiving proton radiotherapy, with the other 2 achieving PRs. At a median follow-up of 22.2 months, 6 of these 7 patients with locoregional ONB who received ID followed by definitive radiotherapy were still alive and the 2-year survival rate was 100%. These findings suggest that induction chemotherapy followed by definitive radiotherapy may be a promising nonsurgical treatment option for patients with locally advanced ONB.

In conclusion, chemotherapy with ID for both advanced and/or metastatic ONB was found to be safe and manageable. The response to ID was no better than expected, however, indicating that ONB requires a more active chemotherapy regimen. Induction chemotherapy followed by proton radiotherapy may be a promising treatment option for patients with locally advanced ONB and warrants further investigation.

REFERENCES

1. Kadish SGM, Wang CC. Olfactory neuroblastoma. A clinical analysis of 17 cases. *Cancer.* 1976;37:1571–1576.
2. Elkon D, Hightower SI, Lim ML, Cantrell RW, Constable WC. Esthesioneuroblastoma. *Cancer.* 1979;44:1087–1094.
3. McCormack LJ, Harris HE. Neurogenic tumors of the nasal fossa. *JAMA.* 1955;157:318–322.
4. Berger L, Luc R. L'esthesioneroepitheliome olfactif. *Bull Assoc Franc Etude Cancer.* 1924;13:410–421.
5. Broich G, Pagliari A, Ottaviani F. Esthesioneuroblastoma: a general review of the cases published since the discovery of the tumour in 1924. *Anticancer Res* 1997;17:2683–2706.
6. Spaulding CA, Kranyak MS, Constable WC, Stewart FM. Esthesioneuroblastoma: a comparison of 2 treatment eras. *Int J Radiat Oncol Biol Phys.* 1988;15:581–590.
7. Resto VA, Eisele DW, Forastiere A, Zahurak M, Lee DJ, Westra WH. Esthesioneuroblastoma: the Johns Hopkins experience. *Head Neck.* 2000;22:550–558.
8. Dulguerov P, Allal AS, Calcaterra TC. Esthesioneuroblastoma: a meta-analysis and review. *Lancet Oncol.* 2001;2:683–690.
9. Austin JR, Cebrun H, Kershisnik MM, et al. Olfactory neuroblastoma and neuroendocrine carcinoma of the anterior skull base: treatment results at the M.D. Anderson Cancer Center. *Skull Base Surg.* 1996;6:1–8.
10. Foote RL, Morita A, Ebersold MJ, et al. Esthesioneuroblastoma: the role of adjuvant radiation therapy. *Int J Radiat Oncol Biol Phys.* 1993;27:835–842.
11. Zappia JJ, Carroll WR, Wolf GT, Thornton AF, Ho L, Krause CJ. Olfactory neuroblastoma: the results of modern treatment approaches at the University of Michigan. *Head Neck.* 1993;15:190–196.
12. Diaz EM Jr, Johnigan RH 3rd, Pero C, et al. Olfactory neuroblastoma: the 22-year experience at 1 comprehensive cancer center. *Head Neck.* 2005;27:138–149.
13. Bhattacharyya N, Thornton AF, Joseph MP, Goodman ML, Amrein PC. Successful treatment of esthesioneuroblastoma and neuroendocrine carcinoma with combined chemotherapy and proton radiation. Results in 9 cases. *Arch Otolaryngol Head Neck Surg.* 1997;123:34–40.
14. Fitzek MM, Thornton AF, Varvares M, et al. Neuroendocrine tumors of the sinonasal tract. Results of a prospective study incorporating chemotherapy, surgery, and combined proton-photon radiotherapy. *Cancer.* 2002;94:2623–2634.
15. Levine PA, Gallagher R, Cantrell RW. Esthesioneuroblastoma: reflections of a 21-year experience. *Laryngoscope.* 1999;109:1539–1543.
16. Miyamoto RC, Gleich LL, Biddinger PW, Gluckman JL. Esthesioneuroblastoma and sinonasal undifferentiated carcinoma: impact of histological grading and clinical staging on survival and prognosis. *Laryngoscope.* 2000;110:1262–125.
17. Simon JH, Zhen W, McCulloch TM, et al. Esthesioneuroblastoma: the University of Iowa experience 1978–1998. *Laryngoscope.* 2001;111:488–493.
18. McElroy EA Jr, Buckner JC, Lewis JE. Chemotherapy for advanced esthesioneuroblastoma: the Mayo Clinic experience. *Neurosurgery.*42:1023–107, 1998; discussion 27–8.
19. Sheehan JM, Sheehan JP, Jane JA, Polin RS. Chemotherapy for esthesioneuroblastomas. *Neurosurg Clin N Am.* 2000;11: 693–701.
20. Goldsweig HG, Sundaresan N. Chemotherapy of recurrent esthesioneuroblastoma. Case report and review of the literature. *Am J Clin Oncol.* 1990;13:139–143.
21. Wade PM Jr, Smith RE, Johns ME. Response of esthesioneuroblastoma to chemotherapy. Report of 5 cases and review of the literature. *Cancer.* 1984;53:1036–1041.
22. Eriksen JG, Bastholt L, Krogdahl AS, Hansen O, Joergensen KE. Esthesioneuroblastoma—what is the optimal treatment? *Acta Oncol.* 2000;39:231–235.
23. Yoh K, Tahara M, Kawada K, et al. Chemotherapy in the treatment of advanced or recurrent olfactory neuroblastoma. *Asia-Pac J Clin Oncol.* 2006;2:180–184.
24. Nishimura H, Ogino T, Kawashima M, et al. Proton-beam therapy for olfactory neuroblastoma. *Int J Radiat Oncol Biol Phys.* 2007;68:758–762.
25. Kawada K, Sasaki Y, Tahara M, et al. Phase I and pharmacokinetic study of weekly docetaxel (DOC) plus irinotecan (IRN) in patients with advanced solid tumors. *Proc Amer Assoc Cancer Res.* 2005;46:938.
26. Silva EG, Butler JJ, Mackay B, Goepfert H. Neuroblastomas and neuroendocrine carcinomas of the nasal cavity. *Cancer.* 1982;50:2388–2405.
27. Mills SE, Frierson HF. Olfactory neuroblastoma: a clinicopathologic study of 21 cases. *Am J Surg Pathol.* 1985;9:317–327.
28. Hyams V, Batsakis J, Michaels L. Tumors of the Upper Respiratory Tract and Ear. 2nd ed. Vol. 25. Washington, DC: Armed Forces Institute of Pathology; 1988.
29. Miller AB, Hoogstraten B, Staquet M, Winkler A. Reporting results of cancer treatment. *Cancer.* 1981;47:207–214.

30. Kaplan E, Meier P. Nonparametric estimation from incomplete observations. *J Am Stat Assoc.* 1958;53:457–481.
31. Morita A, Ebersold MJ, Olsen KD, Foote RL, Lewis JE, Quast LM. Esthesioneuroblastoma: prognosis and management. *Neurosurgery.* 1993;32:706–714; discussion 14–5.
32. Biller HF, Lawson W, Sachdev VP, Som P. Esthesioneuroblastoma: surgical treatment without radiation. *Laryngoscope.* 1990;100:1199–1201.
33. Dulguerov P, Calcaterra T. Esthesioneuroblastoma: the UCLA experience 1970–1990. *Laryngoscope.* 1992;102:843–849.
34. Polin RS, Sheehan JP, Chenelle AG, et al. The role of preoperative adjuvant treatment in the management of esthesioneuroblastoma: the University of Virginia experience. *Neurosurgery.* 1998;42:1029–1037.
35. Chao KS, Kaplan C, Simpson JR, et al. Esthesioneuroblastoma: the impact of treatment modality. *Head Neck.* 2001;23:749–757.
36. Kim DW, Jo YH, Kim JH, et al. Neoadjuvant etoposide, ifosfamide, and cisplatin for the treatment of olfactory neuroblastoma. *Cancer.* 2004;101:2257–2260.
37. Mishima Y, Nagasaki E, Terui Y, et al. Combination chemotherapy (cyclophosphamide, doxorubicin, and vincristine with continuous-infusion cisplatin and etoposide) and radiotherapy with stem cell support can be beneficial for adolescents and adults with esthesioneuroblastoma. *Cancer.* 2004;101:1437–1444.
38. Levine PA, Debo RF, Meredith SD, Jane JA, Constable WC, Cantrell RW. Craniofacial resection at the University of Virginia (1976–1992): survival analysis. *Head Neck.* 1994;16:574–577.
39. Richtsmeier W, Briggs R, Koch W. Complications and early outcome of anterior craniofacial resection. *Arch Otolaryngol Head Neck Surg.* 1992;118:913–917.

0090-9556/07/3510-1865–1872$20.00
DRUG METABOLISM AND DISPOSITION
Copyright © 2007 by The American Society for Pharmacology and Experimental Therapeutics
DMD 35:1865–1872, 2007

Vol. 35, No. 10
15339/3257496
Printed in U.S.A.

Haplotypes and a Novel Defective Allele of *CES2* Found in a Japanese Population

Su-Ryang Kim, Kimie Sai, Toshiko Tanaka-Kagawa, Hideto Jinno, Shogo Ozawa, Nahoko Kaniwa, Yoshiro Saito, Akira Akasawa, Kenji Matsumoto, Hirohisa Saito, Naoyuki Kamatani, Kuniaki Shirao, Noboru Yamamoto, Teruhiko Yoshida, Hironobu Minami, Atsushi Ohtsu, Nagahiro Saijo, and Jun-ichi Sawada

Project Team for Pharmacogenetics (S.-R.K., K.Sa., H.J., S.O., N.Kan., Y.S., J.S.), Division of Biosignaling (K.Sa.), Division of Environmental Chemistry and Exposure Assessment (T.T.-K., H.J.), Division of Pharmacology (S.O.), Division of Medicinal Safety Sciences (N.Kan.), Division of Biochemistry and Immunochemistry (Y.S., J.S.), National Institute of Health Sciences, Tokyo, Japan; Department of Allergy and Immunology, National Research Institute for Child Health and Development (K.M., H.S.), National Children's Medical Center (A.A.), National Center for Child Health and Development, Tokyo, Japan; Division of Genomic Medicine, Department of Advanced Biomedical Engineering and Science, Tokyo Women's Medical University, Tokyo, Japan (N.Kam.); Division of Internal Medicine (K.Sh., N.Y.), National Cancer Center Hospital, Genetics Division (T.Y.), National Cancer Center Research Institute, Tokyo, Japan; and Division of Oncology/Hematology (H.M.), Division of GI Oncology/Digestive Endoscopy (A.O.), Deputy Director (N.S.), National Cancer Center Hospital East, Chiba, Japan

Received February 23, 2007; accepted July 17, 2007

ABSTRACT:

Human carboxylesterase 2 (hCE-2) is a member of the serine esterase superfamily and is responsible for hydrolysis of a wide variety of xenobiotic and endogenous esters. hCE-2 also activates an anticancer drug, irinotecan (7-ethyl-10-[4-(1-piperidino)-1-piperidino]-carbonyloxycamptothecin, CPT-11), into its active metabolite, 7-ethyl-10-hydroxycamptothecin (SN-38). In this study, a comprehensive haplotype analysis of the *CES2* gene, which encodes hCE-2, in a Japanese population was conducted. Using 21 single nucleotide polymorphisms (SNPs), including 4 nonsynonymous SNPs, 100C>T ($Arg^{34}Trp$, *2), 424G>A ($Val^{142}Met$, *3), 1A>T ($Met^{1}Leu$, *5), and 617G>A ($Arg^{206}His$, *6), and a SNP at the splice acceptor site of intron 8 (IVS8-2A>G, *4), 20 haplotypes were identified in 262 Japanese subjects. In 176 Japanese cancer patients who received irinotecan, associations of *CES2* haplotypes and changes in a pharmacokinetic parameter, (SN-38 + SN-38G)/CPT-11 area under the plasma concentration curve (AUC) ratio, were analyzed. No significant association was found among the major haplotypes of the **1* group lacking nonsynonymous or defective SNPs. However, patients with nonsynonymous SNPs, 100C>T ($Arg^{34}Trp$) or 1A>T ($Met^{1}Leu$), showed substantially reduced AUC ratios. In vitro functional characterization of the SNPs was conducted and showed that the 1A>T SNP affected translational but not transcriptional efficiency. These findings are useful for further pharmacogenetic studies on CES2-activated prodrugs.

Human carboxylesterases are members of the serine esterase superfamily and are responsible for hydrolysis of a wide variety of xenobiotic and endogenous esters. They metabolize esters, thioesters, carbamates, and amides to yield soluble acids and alcohols or amines (Satoh and Hosokawa, 1998; Satoh et al., 2002). In the human liver, two major isoforms of carboxylesterase, hCE-1 and hCE-2, have been identified (Shibata et al., 1993; Schwer et al., 1997). hCE-2 is a 60-kDa monomeric enzyme with a pI value of approximately 4.9 and shares 48% amino acid sequence identity with hCE-1 (Pindel et al., 1997; Schwer et al., 1997; Takai et al., 1997). The *CES2* gene, which encodes hCE-2, is located on chromosome 16q22.1 and consists of 12 exons. Distribution of hCE-2 is relatively limited to several tissues, such as the small intestine, colon, heart, kidney, and liver, whereas hCE-1 is ubiquitously expressed (Satoh et al., 2002; Xie et al., 2002).

Although both hCE-1 and hCE-2 show broad substrate specificities, hCE-2 is relatively specific for heroin, cocaine (benzoyl ester), 6-acetylmorphine, procaine, and oxybutynin (Pindel et al., 1997; Takai et al., 1997; Satoh et al., 2002). In addition, hCE-2 is reported to play a major role in the metabolic activation of the antitumor drug irinotecan (7-ethyl-10-[4-(1-piperidino)-1-piperidino]-carbonyloxycamptothecin; CPT-11). Irinotecan is a water-soluble derivative of the plant alkaloid camptothecin and is widely used for treatment of several types of cancer. Irinotecan is converted to 7-ethyl-10-hydroxy-

This study was supported in part by the Program for the Promotion of Fundamental Studies in Health Sciences from the National Institute of Biomedical Innovation and by a Health and Labour Science Research Grant from the Ministry of Health, Labour and Welfare of Japan.

Article, publication date, and citation information can be found at http://dmd.aspetjournals.org.

doi:10.1124/dmd.107.015339.

ABBREVIATIONS: hCE-1, human carboxylesterase 1; hCE-2, human carboxylesterase 2 (EC 3.1.1.1); irinotecan, 7-ethyl-10-[4-(1-piperidino)-1-piperidino]-carbonyloxycamptothecin, CPT-11; SN-38, 7-ethyl-10-hydroxycamptothecin; SN-38G, SN-38 glucuronide; SNP, single nucleotide polymorphisms; PCR, polymerase chain reaction; LD, linkage disequilibrium; 5-FU, 5-fluorouracil; MMC, mitomycin C; AUC, area under plasma concentration curve; RT, reverse transcriptase; UTR, untranslated region; ORF, open reading frame.

camptothecin (SN-38), a topoisomerase inhibitor, by carboxylesterases (Humerickhouse et al., 2000) and further conjugated by hepatic uridine diphosphate glucuronosyltransferase to form the inactive metabolite SN-38 glucuronide (SN-38G) (Iyer et al., 1998). To a lesser extent, irinotecan is also converted to 7-ethyl-10-[4-*N*-(5-aminopentanoic acid)-1-piperidino]carbonyloxycamptothecin and 7-ethyl-10-(4-amino-1-piperidino)carbonyloxycamptothecin by cytochrome P450 3A4 (Dodds et al., 1998; Santos et al., 2000). Irinotecan and its metabolites are excreted by the efflux transporters, ABCB1 (P-glycoprotein), ABCC2 (canalicular multispecific organic anion transporter), and ABCG2 (breast cancer resistance protein), via a hepatobiliary pathway (Mathijssen et al., 2001). Although irinotecan metabolism is rather complex, hCE-2 is a key enzyme that determines the plasma levels of the active metabolite SN-38.

Hepatic hCE-2 activity toward irinotecan varies 3-fold in microsomes obtained from a panel of human livers (Xu et al., 2002). The activity loosely correlates with hCE-2 protein levels, but some microsomal samples showed unanticipated deviating activities. This result might be caused by genetic polymorphisms, such as single nucleotide polymorphisms (SNPs) in the *CES2* gene. Several SNPs and haplotypes have been reported for the *CES2* gene (Charasson et al., 2004; Marsh et al., 2004; Wu et al., 2004), and large ethnic differences in *CES2* SNP frequencies are found among Europeans, Africans, and Asian-Americans (Marsh et al., 2004).

Previously, 12 exons and their flanking regions of *CES2* were sequenced from 153 Japanese subjects, who received irinotecan or steroidal drugs, and 12 novel SNPs, including the nonsynonymous SNP, 100C>T ($Arg^{34}Trp$), and the SNP at the splice acceptor site of intron 8 (IVS8-2A>G) were found (Kim et al., 2003). In vitro functional characterization of these SNPs and an additional nonsynonymous SNP, 424G>A ($Val^{142}Met$), suggested that the ^{34}Trp and ^{142}Met variants were defective, and that IVS8-2G might be a low-activity allele (Kubo et al., 2005). In the present study, the same regions were sequenced from an additional 109 subjects (a total of 262 patients), and their haplotypes/diplotypes were determined/inferred. Then, associations between the haplotypes and pharmacokinetic parameters of irinotecan and its metabolites were analyzed for 177 cancer patients who were given irinotecan. Functional characterization of novel SNPs 1A>T and 617G>A, which were found in this study, was also performed by using a transient expression system with COS-1 cells.

Materials and Methods

Chemicals. Irinotecan, SN-38, and SN-38G were kindly supplied by Yakult Honsha Co. Ltd. (Tokyo, Japan).

Patients. A total of 262 Japanese subjects analyzed in this study consisted of 85 patients with allergies who received steroidal drugs and 177 patients with cancer who received irinotecan. The ethical review boards of the National Cancer Center, National Center for Child Health and Development, and National Institute of Health Sciences approved this study. Written informed consent was obtained from all participants.

DNA Sequencing. Total genomic DNA was extracted from blood leukocytes or Epstein-Barr virus-transformed lymphocytes and used as a template in the polymerase chain reaction (PCR). Sequence data of the *CES2* gene from 72 patients and 81 cancer patients were described previously (Kim et al., 2003). In addition, the *CES2* gene was sequenced from 13 allergic patients and 96 cancer patients. Amplification and sequencing of the *CES2* gene were performed as described previously (Kim et al., 2003). Rare SNPs found in only one heterozygous subject were confirmed by sequencing PCR fragments produced by amplification with a high-fidelity DNA polymerase KOD-Plus (Toyobo, Tokyo, Japan). GenBank accession number NT_010498.15 was used as the reference sequence.

Linkage Disequilibrium and Haplotype Analyses. LD analysis was performed by the SNPAlyze software (version 5.1; Dynacom Co., Yokohama, Japan), and a pairwise two-dimensional map between SNPs was obtained for the D' and rho square (r^2) values. All allele frequencies were in Hardy-Weinberg equilibrium. Some haplotypes were unambiguously assigned in the subjects with homozygous variations at all sites or a heterozygous variation at only one site. Separately, the diplotype configurations (combinations of haplotypes) were inferred by LDSUPPORT software, which determines the posterior probability distribution of the diplotype configuration for each subject on the basis of estimated haplotype frequencies (Kitamura et al., 2002). The haplotype groups were numbered according to the allele nomenclature systems suggested by Nebert (2000). The haplotypes harboring nonsynonymous or defective alleles were assigned as haplotype groups **2* to **6*. The subgroups were described as the numbers plus small alphabetical letters.

Administration of Irinotecan and Pharmacokinetic Analysis. The demographic data and eligibility criteria for 177 cancer patients who received irinotecan in the National Cancer Center Hospitals (Tokyo and Chiba, Japan) were described elsewhere (Minami et al., 2007).

Each patient received a 90-min i.v. infusion at doses of 60 to 150 mg/m^2, which varied depending on regimens/coadministered drugs: i.e., irinotecan dosages were 100 or 150 mg/m^2 for monotherapy and combination with 5-FU, 150 mg/m^2 for combination with mitomycin C (MMC), and 60 (or 70) mg/m^2 for combination with platinum anticancer drugs. Heparinized blood was collected before administration of irinotecan and at 0 min (end of infusion), 20 min, 1 h, 2 h, 4 h, 8 h, and 24 h after infusion. Plasma concentrations of irinotecan, SN-38, and SN-38G were determined as described previously (Sai et al., 2002). The AUCs from time 0 to infinity of irinotecan and its metabolites were calculated as described (Sai et al., 2004). Associations between genotypes and pharmacokinetic parameters including the AUC ratio (SN-38 + SN-38G)/CPT-11 were evaluated in 176 patients in whom pharmacokinetic parameters were obtained.

Construction of Expression Plasmids. The coding region of CES2L (long form) cDNA starts at an additional ATG translation initiation codon located 192 nucleotides upstream of the conventional ATG codon (Wu et al., 2003) and encodes a 623-amino acid protein found in the National Center for Biotechnology Information database (NP_003860.2). The wild-type CES2L cDNA was amplified by PCR from Human Liver QUICK-Clone cDNA (Clontech, Mountain View, CA) using *CES2*-specific primers, 5′-CACCCACCTATGACTGCTCA-3′ and 5′-AGGGAGCTACAGCTCTGTGT-3′. The PCR was performed with 1 unit of the high-fidelity DNA polymerase KOD-Plus and a 0.5 μM concentration of the *CES2* specific primers. The PCR conditions were 94°C for 2 min, followed by 35 cycles of 94°C for 30 s, 60°C for 30 s, and 68°C for 3 min and then a final extension at 68°C for 5 min. The PCR products were cloned into the pcDNA3.1 vector by a directional TOPO cloning procedure (Invitrogen, Carlsbad, CA), and the sequences were confirmed in both directions. The resultant plasmid was designated pcDNA3.1/CES2L-WT. The 1A>T variation was introduced into pcDNA3.1/CES2L-WT by using a QuikChange Multi site-directed mutagenesis kit (Stratagene, La Jolla, CA) with the 5′-phosphorylated oligonucleotide, 5′-phospho-GAGACCAGCGAGCCGACCTTGCGGCTGCACAGACTTCG-3′ (the substituted nucleotide is underlined). The sequence of the variant cDNA was confirmed in both strands, and the resultant plasmid was designated pcDNA3.1/CES2L-A1T. Expression plasmids for the short-form wild-type (CES2S) and $Arg^{206}His$ variant CES2 were prepared and introduced into COS-1 cells according to the method described previously (Kubo et al., 2005).

Expression of Wild-Type and Variant CES2 Proteins in COS-1 Cells. Expression of wild-type and variant CES2 proteins in COS-1 cells was examined as described previously (Kubo et al., 2005). In brief, microsomal fractions (30 μg of protein/lane) or postmitochondrial fractions (0.4 μg of protein/lane) were separated by 8% SDS-polyacrylamide gel electrophoresis and transferred onto a nitrocellulose membrane. Immunochemical detection of each type of CES2 protein was performed using rabbit anti-human CES2 antibody raised against a peptide antigen (residues 539–555, KKALPQKIQELEEPEER) (diluted 1:1500). To verify that the samples were evenly loaded, the blot was subsequently treated with a stripping buffer and reprobed with polyclonal anti-calnexin antibody (diluted 1:2000; Stressgen Biotechnologies Corp., San Diego, CA). Visualization of these proteins was achieved with horseradish peroxidase-conjugated donkey anti-rabbit IgG (1:4000) and the Western Lightning Chemiluminescence Reagent Plus (PerkinElmer Life and Analytical Sciences, Boston, MA). Protein band densities were quantified with Diana III

and ZERO-Dscan software (Raytest, Straubenhardt, Germany). The relative expression levels are shown as the means ± S.D. of three separate transfection experiments.

Determination of CES2 mRNA by Real-Time RT-PCR. Total RNA was isolated from transfected COS-1 cells using the RNeasy Mini Kit (QIAGEN, Tokyo, Japan). After RNase-free DNase treatment of samples to minimize plasmid DNA contamination, first-strand cDNA was prepared from 1 μg of total RNA using the High-Capacity cDNA Archive Kit (Applied Biosystems, Foster City, CA) with random primers. Real-time PCR assays were performed with the ABI7500 Real Time PCR System (Applied Biosystems) using the TaqMan Gene Expression Assay for *CES2* (Hs01077945_m1; Applied Biosystems) according to the manufacturer's instructions. The relative mRNA levels were determined using calibration curves obtained from serial dilutions of the pooled wild-type CES2 cDNA. Samples without reverse transcriptase were routinely included in the RT-PCR reactions to measure possible contributions of contaminating DNA, which was usually less than 1% of the mRNA-derived amplification. Transcripts of β-actin were quantified as internal controls using TaqMan β-Actin Control Reagent (Applied Biosystems), and normalization of CES2 mRNA levels were based on β-actin concentrations.

Enzyme Assay. CPT-11 hydrolyzing activity of the postmitochondrial supernatants (microsomal fraction plus cytosol) was assayed over the substrate concentration range of 0.25 to 50 μM as described previously (Kubo et al., 2005), except that the hydrolysis product, SN-38, was determined by the high-performance liquid chromatography method of Hanioka et al. (2001).

Statistical Analysis. Statistical analysis of the differences in the AUC ratios among *CES2* diplotypes, coadministered drugs. or irinotecan dosages was performed using the Kruskal-Wallis test, Mann-Whitney test, or Spearman rank correlation test (Prism 4.0, GraphPad Software, Inc., San Diego, CA). The *t* test (Prism 4.0) was applied to the comparison of the average values of protein expression and mRNA levels between wild-type and variant CES2.

Results

***CES2* Variations Detected in a Japanese Population.** Previously, the promoter region, all 12 exons, and their flanking introns of the *CES2* gene were sequenced from 72 allergic patients and 81 cancer patients and resulted in the identification of 12 novel SNPs (Kim et al., 2003). Additionally, the same region of *CES2* was sequenced from 13 allergic patients and 96 cancer patients. A total of 21 SNPs were found in 262 Japanese subjects (Table 1). Novel SNPs found in this study were −1233T>C, 1A>T, IVS2-71C>G, IVS7 + 27G>A, and IVS9 + 78C>T, but their frequency was low (0.002, identified in a single heterozygous subject for each SNP). The SNP 1A>T is nonsynonymous (M1L) and results in a substitution of the translation initiation codon ATG to TTG in the *CES2* gene. The other novel SNPs were located in the introns or the 5′-flanking region.

The nonsynonymous SNP 424G>A (V142M) reported by our group (Kubo et al., 2005) and another nonsynonymous SNP 617G>A (R206H) published in the dbSNP (rs8192924) and JSNP (ssj0005417) databases were found at a frequency of 0.002. Recently, several noncoding SNPs in *CES2* were also reported (Kim et al., 2003; Charasson et al., 2004; Marsh et al., 2004; Wu et al., 2004). Among them, the three SNPs, −363C>G in the 5′-UTR, IVS10-108(IVS10 + 406)G>A in intron 10, and 1749(*69)A>G in the 3′-UTR of exon 12, were found at frequencies of 0.031, 0.269, and 0.239, respectively, in this study.

LD and Haplotype Analysis. Using the detected SNPs, LD analysis was performed, and the pairwise values of r^2 and D' were obtained. A perfect linkage (r^2 = 1.00) was observed between SNPs −363C>G and IVS10-87G>A. A close association (r^2 = 0.85) was found between SNPs IVS10-108G>A and 1749A>G. Other associations were much lower (r^2 < 0.1). Therefore, the entire *CES2* gene was analyzed as one LD block. The determined/inferred haplotypes are summarized in Fig. 1 and are shown as numbers plus small

TABLE 1

Summary of SNPs in the CES2 gene in a Japanese population

SNP Identification			Location	Position		Nucleotide Change and Flanking Sequences (5′ to 3′)	Amino Acid Change	Allele Frequency
This Study	NCBI (dbSNP)	JSNP		NT_010498.15	From the Translational Initiation Site or from the Nearest Exon			
MPJ6_CS2001			5′-Flanking	20582067	−1671[a]	CTGGAACAACTCG/CCTCCCCTCGGAA		0.010
MPJ6_CS2002			5′-Flanking	20582484	−1254[a]	AACCACCACCGCT/CGATCCTAGCAGG		0.002
MPJ6_CS2016[b]			5′-Flanking	20582505	−1233[a]	CAGGCGTGCGCTT/CCCGCTCCAACCC		0.002
MPJ6_CS2003			Exon 1 (5′-UTR)	20582979	−759[a]	AAATGTTTGTCAA/GGTGGATAAATGA		0.006
MPJ6_CS2004	rs11075646		Exon 1 (5′-UTR)	20583375	−363[a]	CCTCCTATCGATC/GCCCCAGCGCGCT		0.031
MPJ6_CS2017[b]			Exon 1	20583738	1[a]	AGCGAGCCGACCA/TTGCGGCTGCACA	Met[1]Leu	0.002
MPJ6_CS2005			Exon 2	20586162	100[a]	GCCAGTCCCATCC/TGGACCACACACA	Arg[34]Trp	0.002
MPJ6_CS2021[b]			Intron 2	20587248	IVS2–71	GGTGGCTGGGAGC/GACCTCTGAACCC		0.002
MPJ6_CS2015			Exon 4	20588325	424[a]	TGATTTCCCCAGG/ATGATGGTGTGGA	Val[142]Met	0.002
MPJ6_CS2006			Intron 4	20588486	IVS4 + 29	GCTGGGCAACCCG/AGGCTGAGCGGGG		0.002
MPJ6_CS2007			Exon 5	20588560	579[a]	CAAGCACGCAACC/TGGCAACTGGGGC	Thr[193]Thr (silent)	0.002
MPJ6_CS2018	rs8192924	ssj0005417	Exon 5	20588598	617[a]	TGGCTGCACTACG/ACTGGGTCCAGCA	Arg[206]His	0.002
MPJ6_CS2008			Exon 5	20588746	765[a]	CATGGAGAGTGGC/TGTGGCCCTCCTG	Gly[255]Gly (silent)	0.002
MPJ6_CS2009			Intron 5	20589157	IVS5–69	CCTGTTCTTGGCC/TAGGGCCTTGGGC		0.017
MPJ6_CS2019[b]			Intron 7	20589775	IVS7 + 27	AAGCCCACAAGTG/ACCTGGGGAGCCC		0.002
MPJ6_CS2010			Intron 7	20589845	IVS7–25	CCCATCCCCAGCT/AACAGACTCTCTC		0.002
MPJ6_CS2011			Intron 8	20590205	IVS8–2	TCCACCTGGGGTA/GGATGTTGCCTCC	Splicing defect	0.002
MPJ6_CS2020[b]			Intron 9	20590429	IVS9 + 78	ACCTGCTGCTGTC/TCGGGTCAGCACT		0.002
MPJ6_CS2012	rs2241409	IMS-JST1013275	Intron 10	20591293	IVS10–108	GGAAGAAAAGCG/AGAGAAGCAGGAC		0.269
MPJ6_CS2013	rs28382825		Intron 10	20591314	IVS10–87	GGACTGGGGACCG/AAGGTCTCGGGGG		0.031
MPJ6_CS2014	rs8192925	ssj0005418	Exon 12 (3′-UTR)	20592196	1749 (*69)[a]	GTGCCCACACACA/GCCCACTAAGGAG		0.239

[a] A of the conventional translation initiation codon ATG in *CES2* (GenBank Y09616) is numbered 1, and the number in the parentheses indicates the position from the termination codon TGA.
[b] Novel variations detected in this study.

Position	5'-flanking	5'-flanking	5'-flanking	5'-UTR	5'-UTR	Exon 1	Exon 2	Intron 2	Exon 4	Intron 4	Exon 5	Exon 5	Exon 5	Intron 5	Intron 7	Intron 7	Intron 8	Intron 9	Intron 10	Intron 10	3'-UTR
Nucleotide change	-1671 G>C	-1254 T>G	-1233 T>C	-759 A>G	-383 C>G	1 A>T	100 C>T	IVS2-71 C>G	424 G>A	IVS4+29 G>A	579 C>T	617 G>A	785 C>T	IVS5-69 C>T	IVS7+27 G>A	IVS7-25 T>A	IVS8-2 A>G	IVS9+85 C>T	IVS10-108 G>A	IVS10-87 G>A	1749(+69) A>G
Effect on protein						M1L	R34W		V142M		T193T (silent)	R206H	G255G (silent)				splicing defect				

Haplotype group	Haplotype	Number	Frequency	
*1	*1a	357	0.681	0.990
	*1b	122	0.233	
	*1c	14	0.027	
	*1d	9	0.017	
	*1e	5	0.010	
	*1f	3	0.006	
	*1g	1	0.002	
	*1h	1	0.002	
	*1i	1	0.002	
	*1j	1	0.002	
	*1k	1	0.002	
	*1l	1	0.002	
	*1m#	1	0.002	
	*1n#	1	0.002	
	*1o#	1	0.002	
*2	*2a	1	0.002	0.002
*3	*3a	1	0.002	0.002
*4	*4a	1	0.002	0.002
*5	*5a	1	0.002	0.002
*6	*6a#	1	0.002	0.002
		Total 524	1.000	1.000

FIG. 1. Haplotypes of the *CES2* gene assigned for 262 Japanese subjects. The haplotypes assigned are described with lower case numbers and alphabetical letters. #, this haplotype was inferred in only one patient and is thus ambiguous.

alphabetical letters. Our nomenclature of haplotypes is distinct from those of previous studies (Charasson et al., 2004; Marsh et al., 2004; Wu et al., 2004). In this study, the haplotypes without amino acid changes and splicing defects were defined as the **1* group. The haplotypes harboring the nonsynonymous SNPs, 100C>T ($Arg^{34}Trp$), 424G>A ($Val^{142}Met$), 1A>T ($Met^{1}Leu$), and 617G>A ($Arg^{206}His$), were assigned as haplotypes **2*, **3*, **5*, and **6*, respectively. In addition, the haplotype harboring a SNP at the splice acceptor site of intron 8 (IVS8-2A>G) was assigned as haplotype **4*. Several haplotypes were first unambiguously assigned by homozygous variations at all sites (**1a* and **1b*) or heterozygous variation at only one site (**1d* to **1l*, **2a*, **3a*, **4a*, and **5a*). Separately, the diplotype configurations (combinations of haplotypes) were inferred by LDSUPPORT software. The additionally inferred haplotypes were **1c* and **1m* to **1o*. The most frequent haplotype was **1a* (frequency, 0.681), followed by **1b* (0.233), **1c* (0.027), and **1d* (0.017). The frequencies of the other haplotypes were less than 0.01.

Association between *CES2* Genotypes and Irinotecan Pharmacokinetics. Next, the relationships between the *CES2* genotype and AUC ratio [(SN-38 + SN-38G)/CPT-11], a parameter of in vivo CES activity (Cecchin et al., 2005), in irinotecan-administered patients were investigated. The diplotype distribution of 176 patients, who received irinotecan and were analyzed for the AUC ratio, was similar to that of the 262 subjects. We examined preliminarily the effects of irinotecan dosage and comedication on the AUC ratio and obtained significant correlations of irinotecan dosage (Spearman $r = -0.559$, $p < 0.0001$) and comedication ($p < 0.0001$, Kruskal-Wallis test) with the AUC ratios. Because irinotecan dosages also depended on the drugs coadministered (see *Materials and Methods*), we finally stratified the patients with the coadministered drugs. As shown in Fig. 2, no significant differences in the median AUC ratios were observed among the **1* diplotypes in each group (p values in the Kruskal-Wallis test among **1a/*1a*, **1a/*1b*, and **1b/*1b* were 0.260, 0.470, 0.129, and 0.072 for irinotecan alone, with 5-FU, with MMC and with platinum, respectively.). The relatively rare haplotype **1c*, which harbors −363C>G, did not show any associations with altered AUC ratio ($p = 0.756$ for irinotecan alone and $p = 0.230$ for irinotecan with platinum, Mann-Whitney test).

To estimate the effects of nonsynonymous SNPs on the metabolism of irinotecan, the AUC ratios in the patients carrying nonsynonymous SNPs were compared with the median AUC ratio of the **1/*1* patients. Three nonsynonymous SNPs, 100C>T ($Arg^{34}Trp$, **2*), 1A>T ($Met^{1}Leu$, **5*), and 617G>A ($Arg^{206}His$, **6*), and a SNP at the splice acceptor site of intron 8 (IVS8-2A>G, **4*) were found in 177 patients who received irinotecan. These SNPs were single heterozygotes. The AUC ratios of the patients with **2a/*1a* (0.17) and **5a/*1a* (0.10) in the monotherapy group were 60 and 36%, respectively, of the median value for the **1/*1* group (0.28) and substantially lower than the 25th percentile of the **1/*1* group (0.23) (Fig. 2). It must be noted that the **5a/*1a* patient had an extremely low AUC ratio. The AUC ratio of the **6* heterozygote who received cisplatin (0.25) was lower than the median value (0.37) but within the range for the **1/*1* group treated with platinum-containing drugs (Fig. 2). Regarding the effect of the heterozygous **4*, the AUC ratio (0.40) was not different from the median AUC ratio of the **1/*1* treated with platinum-containing drugs. To elucidate the effects of two novel amino acid substitutions, $Met^{1}Leu$ (**5*) and $Arg^{206}His$ (**6*), the functional analysis was conducted in vitro.

In Vitro Functional Analysis of the $Met^{1}Leu$ Variant. To clarify the functional significance of the novel variant $Met^{1}Leu$ (**5*), the protein expression level of CES2 carrying the nonsynonymous SNP 1A>T was examined. Wu et al. (2003) reported that transcription of CES2 mRNA was initiated from several transcriptional start sites, resulting in the expression of three *CES2* transcripts. Two longer transcripts carry a potential inframe translational initiation codon ATG at −192 that can encode an open reading frame (ORF) extending 64 residues at the amino terminus, as shown in the reference sequence in the National Center for Biotechnology Information database (NP_003860.2). Therefore, the expression of the CES2 protein from the long *CES2* ORF (CES2L), which encodes a potential 623 residue protein, was analyzed. Western analysis of membrane fraction proteins obtained from COS-1 cells

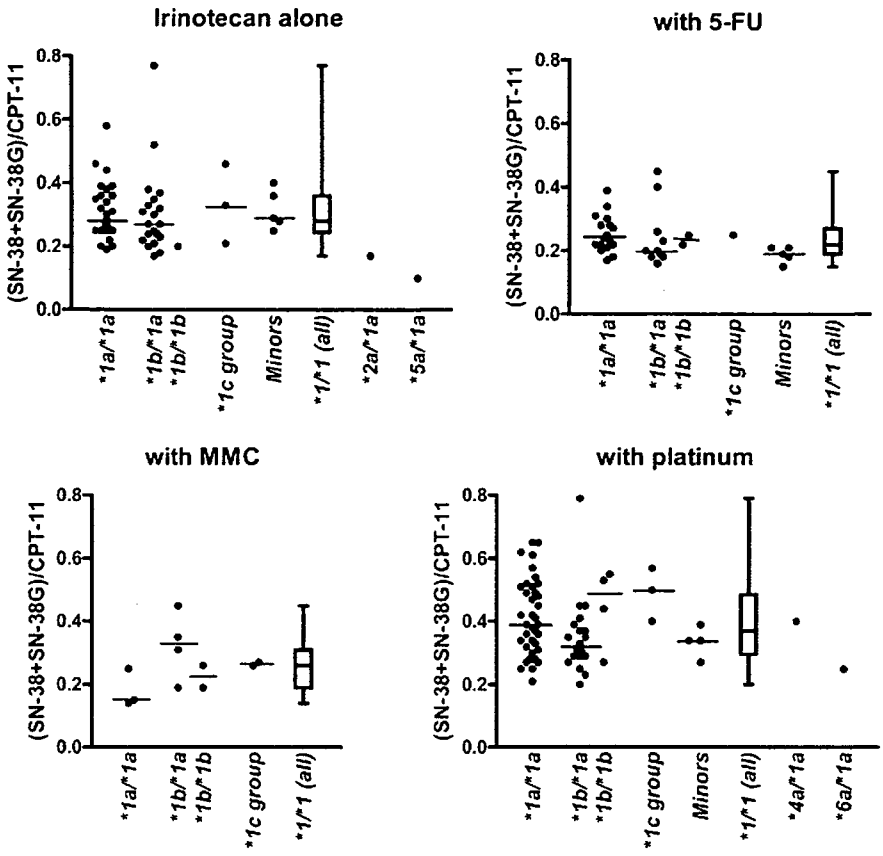

FIG. 2. Relationship between the *CES2* diplotypes and (SN-38 + SN-38G)/CPT-11 AUC ratios in Japanese cancer patients who received irinotecan. Each point represents an individual patient, and the median value in each genotype is shown with a horizontal bar. Distribution of the **1* group is shown by a box representing the 25th to 75th percentiles with a line at the median and bars representing the highest and lowest values. The **1c* group consists of **1c/*1a* and **1c/*1b*. "Minors" represents the heterozygous patients bearing minor **1* haplotypes (**1d, *1e, *1f, *1g, *1k,* and **1m*). Irinotecan alone, irinotecan monotherapy (n = 58); with 5-FU, combination therapy with 5-FU including tegafur (n = 35); with MMC, combination therapy with mitomycin C (n = 11); with platinum, combination therapy with either cisplatin (n = 62), cisplatin plus etoposide (n = 2), or carboplatin (n = 8).

transfected with the expression plasmid pcDNA3.1/CES2L-WT showed that the mobility (approximately 60 kDa) of the protein product from the CES2L cDNA was the same as that from the CES2S cDNA, which encodes a 559 residue protein (Kubo et al., 2005), and the CES2 protein in the human liver microsome (Fig. 3A). Western blot analysis of whole cell extracts also showed that CES2L yielded a single 60-kDa protein product (data not shown), indicating that translation of *CES2* was initiated from the second ATG codon of the *CES2L* ORF but not from the inframe translation initiation codon located at −192.

When the effect of the 1A>T SNP on the expression of the CES2 protein was examined by Western blotting (Fig. 3A), the relative expression levels of CES2 protein from cells transfected with plasmid pcDNA3.1/CES2L-A1T were 11.7 ± 2.4% (p = 0.0003) of the wild type. The mRNA expression levels determined by the TaqMan real-time RT-PCR assay were similar between the wild-type and variant CES2L cDNAs in COS-1 cells (Fig. 4A), indicating that the 1A>T SNP affects translational but not transcriptional efficiency. Thus, the $Met^{1}Leu$ variant was functionally deficient.

In Vitro Functional Analysis of the $Arg^{206}His$ Variant. The known nonsynonymous SNP 617G>A changes an arginine to a histidine at residue 206. Western blot analysis of the postmitochondrial supernatant (including microsomes and cytosol) fractions obtained from COS-1 cells transfected with wild-type (CES2S) and $Arg^{206}His$ variant CES2-expressing plasmids showed that the protein expression level of the $Arg^{206}His$ variant was approximately 82 ± 7% (p = 0.017) of the wild-type (Fig. 3B). No significant differences in the mRNA expression levels determined by the TaqMan real-time RT-PCR assay were observed between the wild-type and 617G>A variant CES2s (82 ± 7%, p = 0.06) (Fig. 4B). Table 2 summarizes the apparent kinetic parameters for CPT-11 hydrolysis of wild-type and $Arg^{206}His$ variant CES2.

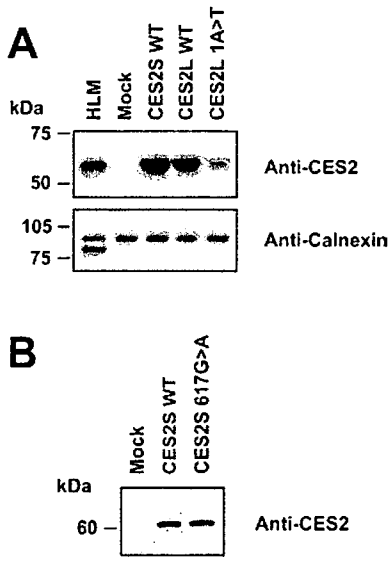

FIG. 3. Expression of CES2 protein from the wild-type and 1A>T (A) and 617G>A (B) variant *CES2* genes in COS-1 cells. Membrane fraction (A) or the postmitochondrial supernatant (B) from the cDNA-transfected cells was subjected to SDS-polyacrylamide gel electrophoresis, followed by transfer to the nitrocellulose membrane. Detection of CES2 and calnexin was performed with rabbit anti-human CES2 antiserum (A and B) and a rabbit anti-human calnexin antiserum (A) and horseradish peroxidase-conjugated donkey anti-rabbit IgG antibody as described under *Materials and Methods*. A representative result from one of three independent experiments is shown. HLM, human liver microsomes.

Although a slight difference in the K_m values was obtained with statistical significance ($p < 0.01$), the kinetic parameters (V_{max} and V_{max}/K_m) were not significantly different when normalized by protein expression levels.

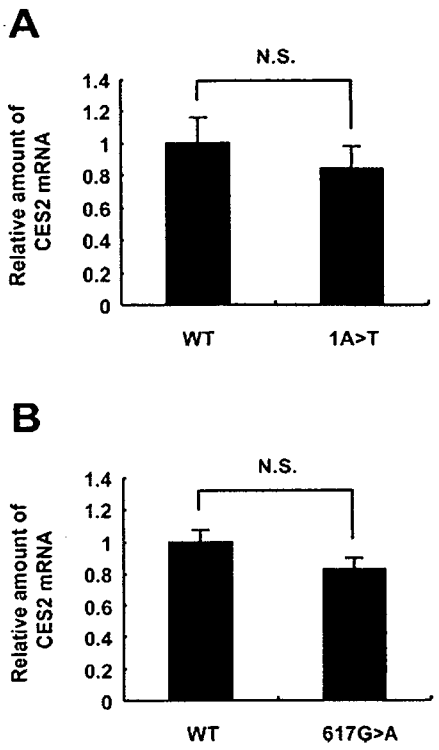

FIG. 4. Quantification of CES2 mRNA by TaqMan real-time RT-PCR in COS-1 cells transfected with wild-type (WT) and 1A>T (A) and 617G>A (B) variants. CES2 mRNA expression levels after 48 h were normalized with β-actin mRNA levels, and the mean level of the wild-type was set as 1.0. The results indicate the mean ± S.D. from three independent preparations. No significant difference in mRNA level was observed between the wild-type and variants ($p = 0.21$ an 0.06 in A and B, respectively).

Discussion

The present study provides comprehensive data on the haplotype analysis of the *CES2* gene, which encodes human carboxylesterase 2. From additional sequence analysis, a total of 21 SNPs including 4 nonsynonymous SNPs, 100C>T ($Arg^{34}Trp$), 424G>A ($Val^{142}Met$), 1A>T ($Met^{1}Leu$), and 617G>A ($Arg^{206}His$), and a SNP at the splice acceptor site of intron 8 (IVS8-2A>G) were found in 262 Japanese subjects. Among the nonsynonymous SNPs, in vitro functional analysis of the two nonsynonymous SNPs, 100C>T ($Arg^{34}Trp$) and 424G>A ($Val^{142}Met$), has already been performed to identify effects of these SNPs on expression levels and carboxylesterase activity. Kubo et al. (2005) showed that $Arg^{34}Trp$ and $Val^{142}Met$ variants had little carboxylesterase activity toward irinotecan, *p*-nitrophenyl acetate, and 4-methylumbelliferyl acetate, whereas expression levels of these variants were higher than those of the wild-type. An in vitro splicing assay using the *CES2* minigene carrying SNP IVS8-2A>G showed that IVS8-2A>G yielded mostly aberrantly spliced transcripts, resulting in the production of truncated CES2 proteins. These results have suggested that 100C>T ($Arg^{34}Trp$), 424G>A ($Val^{142}Met$), and IVS8-2A>G are functionally defective SNPs.

A novel SNP 1A>T found in this study changes the translation start codon ATG to TTG. Wu et al. (2003) identified three transcription start sites of *CES2*, resulting in the synthesis of three transcripts with either 78, 629, or 1187 nucleotides in the 5′-UTR. Another inframe ATG codon is present 192 nucleotides upstream of the conventional translational initiation codon, and two longer transcripts with 629 and 1187 nucleotides in the 5′-UTR can encode an ORF with 64 additional residues at the amino terminus (NP_003860.2). However, as shown in Fig. 3A, our in vitro experiment for the expression of CES2 showed that translation of CES2 mRNA started from the previously reported ATG codon but not from the inframe ATG codon at −192, when transiently expressed from the wild-type *CES2L* cDNA encoding a potential 623-amino acid CES2 protein in COS-1 cells. In vertebrate mRNAs, a purine residue in position −3 (A of the translational start codon is +1) is highly conserved and required for efficient translation (Kozak, 1991). The surrounding sequences of both ATG codons were accATGc for the functional ATG codon and cctATGa for the potential inframe ATG codon at −192. Thus, it is likely that their efficiencies of translation initiation depend on the flanking sequences of the translational start codon ATG.

When the expression levels between the wild-type and 1A>T variant were compared, the protein level of 1A>T was drastically reduced without changes in the mRNA levels, suggesting that the reduced protein level of the 1A>T variant might have been caused by its reduced translation initiation. It has been reported that alterations of the translational start codon ATG to TTG diminish or reduce the translation of growth hormone receptor (Quinteiro et al., 2002), protoporphyrinogen oxidase (Frank et al., 1999), low-density lipoprotein receptor (Langenhoven et al., 1996), and mitochondrial acetoacetyl-CoA thiorase (Fukao et al., 2003). Thus, it is likely that the 1A>T variation is a low-activity variation.

The functional effect of the known nonsynonymous SNP 617G>A ($Arg^{206}His$) was also investigated. The Arg^{206} residue is located in the α-helix within the catalytic domain and conserved among human carboxylesterases (Bencharit et al., 2002). However, no significant differences were found between the intrinsic enzyme activities of the wild-type and $Arg^{206}His$ variant for irinotecan hydrolysis.

In this study, 20 haplotypes of the *CES2* gene were identified. The most frequent haplotype was **1a* (frequency, 0.681), followed by **1b* (0.233), **1c* (0.027), and **1d* (0.017). Haplotype **1b* includes the polymorphisms IVS10-108G>A and 1749A>G, and haplotype **1c* harbors −363C>G, IVS10-108G>A, and IVS10-87G>A. The haplotype corresponding to **1b* in this study was found in Caucasians with a frequency of 0.086 (haplotypes 3 and 7 in Wu et al., 2004). Our **1c* corresponds to haplotypes 2 and 12 in Wu et al. (2004) and genotypes **1* and **6* in Charasson et al. (2004). Among the SNPs consisting of haplotype **1b* and **1c*, the three SNPs, −363C>G in the 5′-UTR, IVS10-108(IVS10 + 406)G>A in intron 10, and

TABLE 2

Kinetic parameters of CPT-11 hydrolysis by wild-type and $Arg^{206}His$ variant CES2 expressed in COS-1 cells

Results are expressed as the mean ± S.D. from four independent transfection experiments.

CES2	Apparent K_m	V_{max}	V_{max}/K_m	Normalized V_{max}[a]	Normalized V_{max}/K_m[a]
	μM	*pmol/min/mg protein*	*nl/min/mg protein*	*pmol/min/mg protein*	*nl/min/mg protein*
Wild-type	0.46 ± 0.01	3.45 ± 0.29	7.43 ± 0.54	3.46 ± 0.23	7.45 ± 0.50
$Arg^{206}His$	0.51 ± 0.02[‡]	2.81 ± 0.22[†]	5.53 ± 0.52[‡]	3.44 ± 0.16	6.77 ± 0.46

[a] V_{max} values were normalized by the relative protein expression level of the $Arg^{206}His$ variant (0.82 ± 0.07).
[†] Significantly different from that of the wild-type at $P < 0.05$.
[‡] $P < 0.01$.

1749(*69)A>G in the 3′-UTR of exon 12, were previously reported, and their frequencies varied among several ethnic groups (Marsh et al., 2004; Wu et al., 2004). The frequency (0.269) of the **1b/*1c*-tagging SNP in Japanese, IVS10-108G>A, was comparable to that in African-Americans (0.263), but much higher than that in Asian-Americans (0.06) and European-Americans (0.063) (Wu et al., 2004). However, the **1b*-tagging SNP 1749A>G (0.239 in this study) was detected only in Asian-Americans with a low frequency (0.03) (Wu et al., 2004). The frequency of the **1c*-tagging SNP, −363C>G, also showed marked ethnic differences between Japanese (0.031) and Europeans (0.12) or Africans (0.33) (our data; Marsh et al., 2004). These findings indicate the existence of large ethnic difference in haplotype structures among African, European, and Japanese populations.

In this study, the relationship between the *CES2* genotypes and the (SN-38 + SN-38G)/CPT-11 AUC ratios of irinotecan-administered patients was analyzed. First, the relationship between the genotypes and the AUC ratios among the **1/*1* diplotypes in the patient group with or without coadministered drugs was assessed, and no significant differences in the AUC ratios were observed among the **1/*1* diplotypes in each group (Fig. 2). Wu et al. (2004) reported that the haplotype harboring SNP −363C>G that was homozygous appeared to have lower mRNA levels than the other haplotype groups. In this study, the haplotype having the SNP −363C>G was assigned haplotype **1c*. However, no functional differences were found between haplotype **1c* and the other **1* group haplotypes. Marsh et al. (2004) reported that IVS10-88C>T was associated with reduced RNA expression in colon tumor tissues. However, this SNP was not found in the present study with Japanese subjects.

The major **1* group haplotypes, **1a*, **1b*, and **1c*, account for 94% of Japanese *CES2* haplotypes. The current study revealed no association between the major *CES2* genotypes and changes in the AUC ratio, indicating that the variability in AUC ratio could not be interpreted by these haplotypes alone.

In irinotecan-administered patients, three nonsynonymous SNPs, 100C>T ($Arg^{34}Trp$, *2), 1A>T ($Met^{1}Leu$, *5), and 617G>A ($Arg^{206}His$, *6), and a SNP at the splice acceptor site of intron 8 (IVS8-2A>G, *4) were found as single heterozygotes. The patients heterozygous for $Arg^{34}Trp$ or $Met^{1}Leu$ showed substantially reduced AUC ratios. These results were consistent with in vitro functional analysis for the nonsynonymous SNPs by Kubo et al. (2005).

In the case of haplotype *6 harboring the nonsynonymous SNP, 617G>A ($Arg^{206}His$), the AUC ratio of the patient who received cisplatin was lower than the median value but within the range for the **1/*1* group treated with platinum-containing drugs. The protein expression level of the 206His variant was 82 ± 4%, and the $Arg^{206}His$ substitution itself showed no functional differences in intrinsic enzyme activity by in vitro functional analysis. Thus, the impact of the 617G>A ($Arg^{206}His$) SNP on irinotecan pharmacokinetics might be small.

On the other hand, the AUC ratio of the patient carrying the haplotype *4 was not different from the median value of the **1/*1* group treated with platinum-containing drugs. It is possible that other genetic factors might have increased the AUC ratio in this patient.

The patients with **4*, **5*, or **6* were found as single heterozygotes. Thus, further studies are needed to elucidate in vivo importance of the three haplotypes.

In conclusion, we have identified a panel of haplotypes of the *CES2* gene in a Japanese population using 21 genetic polymorphisms detected in this study and found that some rare haplotypes with nonsynonymous SNPs show a decreasing tendency toward enzymatic levels or activity. In vitro functional analysis for nonsynonymous SNPs showed that the 1A>T ($Met^{1}Leu$) SNP was a defective allele. These findings will be useful for further pharmacogenetic studies on efficacy and adverse reactions to CES2-activated prodrugs.

Acknowledgments. We thank Chie Sudo for secretarial assistance. We also thank Yakult Honsha Co. Ltd. for kindly providing CPT-11, SN-38, and SN-38G.

References

Bencharit S, Morton CL, Howard-Williams EL, Danks MK, Potter PM, and Pedinbo MR (2002) Structural insight into CPT-11 activation by mammalian carboxylesterases. *Nat Struct Biol* **9**:337–342.

Cecchin E, Corona G, Masier S, Biason P, Cattarossi G, Frustaci S, Buonadonna A, Colussi A, and Toffoli G (2005) Carboxylesterase isoform 2 mRNA expression in peripheral blood mononuclear cells is a predictive marker of the irinotecan to SN38 activation step in colorectal cancer patients. *Clin Cancer Res* **11**:6901–6907.

Charasson V, Bellott R, Meynard D, Longy M, Gorry P, and Robert J (2004) Pharmacogenetics of human carboxylesterase 2, an enzyme involved in the activation of irinotecan into SN-38. *Clin Pharmacol Ther* **76**:528–535.

Dodds HM, Haaz MC, Riou JF, Robert J, and Rivory LP (1998) Identification of a new metabolite of CPT-11 (irinotecan): pharmacological properties and activation to SN-38. *J Pharmacol Exp Ther* **286**:578–583.

Frank J, McGrath JA, Poh-Fitzpatrick MB, Hawk JL, and Christiano AM (1999) Mutations in the translation initiation codon of the protoporphyrinogen oxidase gene underlie variegate porphyria. *Clin Exp Dermatol* **24**:296–301.

Fukao T, Matsuo N, Zhang GX, Urasawa R, Kubo T, Kohno Y, and Kondo N (2003) Single base substitutions at the initiator codon in the mitochondrial acetoacetyl-CoA thiolase (ACAT1/T2) gene result in production of varying amounts of wild-type T2 polypeptide. *Hum Mutat* **21**:587–592.

Hanioka N, Jinno H, Nishimura T, Ando M, Ozawa S, and Sawada J (2001) High-performance liquid chromatographic assay for glucuronidation activity of 7-ethyl-10-hydroxycamptothecin (SN-38), the active metabolite of irinotecan (CPT-11), in human liver microsomes. *Biomed Chromatogr* **15**:328–333.

Humerickhouse R, Lohrbach K, Li L, Bosron WF, and Dolan ME (2000) Characterization of CPT-11 hydrolysis by human liver carboxylesterase isoforms hCE-1 and hCE-2. *Cancer Res* **60**:1189–1192.

Iyer L, King CD, Whitington PF, Green MD, Roy SK, Tephly TR, Coffman BL, and Ratain MJ (1998) Genetic predisposition to the metabolism of irinotecan (CPT-11): role of uridine diphosphate glucuronosyltransferase isoform 1A1 in the glucuronidation of its active metabolite (SN-38) in human liver microsomes. *J Clin Invest* **101**:847–854.

Kim SR, Nakamura T, Saito Y, Sai K, Nakajima T, Saito H, Shirao K, Minami H, Ohtsu A, Yoshida T, et al. (2003) Twelve novel single nucleotide polymorphisms in the *CES2* gene encoding human carboxylesterase 2 (hCE-2). *Drug Metab Pharmacokinet* **18**:327–332.

Kitamura Y, Moriguchi M, Kaneko H, Morisaki H, Morisaki T, Toyama K, and Kamatani N (2002) Determination of probability distribution of diplotype configuration (diplotype distribution) for each subject from genotypic data using the EM algorithm. *Ann Hum Genet* **66**:183–193.

Kozak M (1991) An analysis of vertebrate mRNA sequences: intimations of translational control. *J Cell Biol* **115**:887–903.

Kubo T, Kim SR, Sai K, Saito Y, Nakajima T, Matsumoto K, Saito H, Shirao K, Yamamoto N, Minami H, et al. (2005) Functional characterization of three naturally occurring single nucleotide polymorphisms in the *CES2* gene encoding carboxylesterase 2 (hCE-2). *Drug Metab Dispos* **33**:1482–1487.

Langenhoven E, Warnich L, Thiart R, Rubinsztein DC, van der Westhuyzen DR, Marais AD, and Kotze MJ (1996) Two novel point mutations causing receptor-negative familial hypercholesterolemia in a South African Indian homozygote. *Atherosclerosis* **125**:111–119.

Marsh S, Xiao M, Yu J, Ahluwalia R, Minton M, Freimuth RR, Kwok PY, and McLeod HL (2004) Pharmacogenomic assessment of carboxylesterases 1 and 2. *Genomics* **84**:661–668.

Mathijssen RH, van Alphen RJ, Verweij J, Loos WJ, Nooter K, Stoter G, and Sparreboom A (2001) Clinical pharmacokinetics and metabolism of irinotecan (CPT-11). *Clin Cancer Res* **7**:2182–2194.

Minami H, Sai K, Saeki M, Saito Y, Ozawa S, Suzuki K, Kaniwa N, Sawada J, Hamaguchi T, Yamamoto N, et al. (2007) Irinotecan pharmacokinetics/pharmacodynamics and *UGT1A* genetic polymorphisms in Japanese: roles of *UGT1A1*6* and **28*. *Pharmacogenet Genomics* **17**:497–504.

Nebert DW (2000) Suggestions for the nomenclature of human alleles: relevance to ecogenetics, pharmacogenetics and molecular epidemiology. *Pharmacogenetics* **10**:279–290.

Pindel EV, Kedishvili NY, Abraham TL, Brzezinski MR, Zhang J, Dean RA, and Bosron WF (1997) Purification and cloning of a broad substrate specificity human liver carboxylesterase that catalyzes the hydrolysis of cocaine and heroin. *J Biol Chem* **272**:14769–14775.

Quinteiro C, Castro-Feijoo L, Loidi L, Barreiro J, de la Fuente M, Dominguez F, and Pombo M (2002) Novel mutation involving the translation initiation codon of the growth hormone receptor gene (GHR) in a patient with Laron syndrome. *J Pediatr Endocrinol Metab* **15**:1041–1045.

Sai K, Kaniwa N, Ozawa S, and Sawada J (2002) An analytical method for irinotecan (CPT-11) and its metabolites using a high-performance liquid chromatography: parallel detection with fluorescence and mass spectrometry. *Biomed Chromatogr* **16**:209–218.

Sai K, Saeki M, Saito Y, Ozawa S, Katori N, Jinno H, Hasegawa R, Kaniwa N, Sawada J, Komamura K, et al. (2004) UGT1A1 haplotypes associated with reduced glucuronidation and increased serum bilirubin in irinotecan-administered Japanese patients with cancer. *Clin Pharmacol Ther* **75**:501–515.

Santos A, Zanetta S, Cresteil T, Deroussent A, Pein F, Raymond E, Vernillet L, Risse ML, Boige V, Gouyette A, et al. (2000) Metabolism of irinotecan (CPT-11) by CYP3A4 and CYP3A5 in humans. *Clin Cancer Res* **6**:2012–2020.

Satoh T and Hosokawa M (1998) The mammalian carboxylesterases: from molecules to functions. *Annu Rev Pharmacol Toxicol* **38**:257–288.

Satoh T, Taylor P, Bosron WF, Sanghani SP, Hosokawa M, and LaDu BN (2002) Current progress on esterases: from molecular structure to function. *Drug Metab Dispos* **30**:488–493.

Schwer H, Langmann T, Daig R, Becker A, Aslanidis C, and Schmit G (1997) Molecular cloning and characterization of a novel putative carboxylesterase, present in human intestine and liver. *Biochem Biophys Res Commun* **233**:117–120.

Shibata F, Takagi Y, Kitajima M, Kuroda T, and Omura T (1993) Molecular cloning and characterization of a human carboxylesterase gene. *Genomics* **17**:76–82.

Takai S, Matsuda A, Usami Y, Adachi T, Sugiyama T, Katagiri Y, Tatematsu M, and Hirano K (1997) Hydrolytic profile for ester- or amide-linkage by carboxylesterases pI 5.3 and 4.5 from human liver. *Biol Pharm Bull* **20**:869–873.

Wu MH, Chen P, Remo BF, Cook EH Jr, Das S, and Dolan ME (2003) Characterization of multiple promoters in the human carboxylesterase 2 gene. *Pharmacogenetics* **13**:425–435.

Wu MH, Chen P, Wu X, Liu W, Strom S, Das S, Cook EH Jr, Rosner GL, and Dolan ME (2004) Determination and analysis of single nucleotide polymorphisms and haplotype structure of the human carboxylesterase 2 gene. *Pharmacogenetics* **14**:595–605.

Xie M, Yang D, Liu L, Xue B, and Yan B (2002) Human and rodent carboxylesterases: immunorelated-ness, overlapping substrate specificity, differential sensitivity to serine enzyme inhibitors, and tumor-related expression. *Drug Metab Dispos* **30**:541–547.

Xu G, Zhang W, Ma MK, and McLeod HL (2002) Human carboxylesterase 2 is commonly expressed in tumor tissue and is correlated with activation of irinotecan. *Clin Cancer Res* **8**:2605–2611.

Address correspondence to: Dr. Su-Ryang Kim, Project Team for Pharmacogenetics, National Institute of Health Sciences, 1-18-1 Kamiyoga, Setagaya-ku, Tokyo 158-8501, Japan. E-mail: kim@nihs.go.jp

Phase I and II pharmacokinetic and pharmacodynamic study of the proteasome inhibitor bortezomib in Japanese patients with relapsed or refractory multiple myeloma

Yoshiaki Ogawa,[1,4] Kensei Tobinai,[2] Michinori Ogura,[3] Kiyoshi Ando,[1] Takahide Tsuchiya,[1] Yukio Kobayashi,[2] Takashi Watanabe,[2] Dai Maruyama,[2] Yasuo Morishima,[3] Yoshitoyo Kagami,[3] Hirofumi Taji,[3] Hironobu Minami,[4] Kuniaki Itoh,[4] Masanobu Nakata[4] and Tomomitsu Hotta[1]

[1]Department of Hematology and Oncology, Tokai University School of Medicine, 143, Shimokasuya, Isehara, Kanagawa, 259-1193; [2]Hematology and Stem Cell Transplantation Division, National Cancer Center Hospital, 5-1-1, Tsukiji, Chuo-ku, Tokyo, 104-0045; [3]Department of Hematology and Cell Therapy, Aichi Cancer Center, 1-1, Kanokoden, Chikusa-ku, Nagoya, Aichi, 464-8681; [4]Division of Oncology and Hematology, National Cancer Center Hospital East, 6-5-1, Kashiwanoha, Kashiwa, Chiba, 277-8577, Japan

(Received July 22, 2007/Revised September 6, 2007/Accepted September 9, 2007/Online publication October 29, 2007)

The purpose of this phase I and II study was to evaluate the safety, pharmacokinetics, pharmacodynamics, and efficacy of bortezomib in Japanese patients with relapsed or refractory multiple myeloma. This was a dose-escalation study designed to determine the recommended dose for Japanese patients (phase I) and to investigate the antitumor activity and safety (phase II) of bortezomib administered on days 1, 4, 8, and 11 every 21 days. Thirty-four patients were enrolled. A dose-limiting toxicity was febrile neutropenia, which occurred in one of six patients in the highest-dose cohort in phase I and led to the selection of 1.3 mg/m^2 as the recommended dose. Adverse events ≥ grade 3 were rare except for hematological toxicities, although there was one fatal case of interstitial lung disease. The overall response rate was 30% (95% confidence interval, 16–49%). Pharmacokinetic evaluation showed a biexponential decline, characterized by a rapid distribution followed by a longer elimination, after dose administration, whereas the area under the concentration–time curve increased proportionately with the dose. Bortezomib was effective in Japanese patients with relapsed or refractory multiple myeloma. A favorable tolerability profile was also seen, although the potential for pulmonary toxicity should be monitored closely. The pharmacokinetic and pharmacodynamic profiles of bortezomib in the present study warrant further investigations, including more relevant administration schedules. (*Cancer Sci* 2008; 99: 140–144)

Multiple myeloma, one of the B-cell lymphatic tumors, is a malignant hematopoietic tumor with poor prognosis for which a cure cannot ever be expected. The peak age of onset is high at 65–70 years, and its onset in patients younger than 40 years is rare. The median survival of patients with multiple myeloma is approximately 6–12 months if untreated, but it is prolonged to approximately 3 years with the administration of chemotherapy; the 5-year survival rate has been reported to be approximately 25% and the 10-year survival rate is <5%.[1,2] As initial therapy for multiple myeloma, melphalan + prednisolone therapy and vincristine + doxorubicin + dexamethasone therapy have been used as global standards.[3,4] High-dose chemotherapy combined with autologous hematopoietic stem-cell transplantation is reported to be significantly superior to multiagent chemotherapy in terms of response rate and progression-free survival,[5] and is considered to be a standard therapy primarily for patients who are 65 years old or younger. However, no consensus has been reached on the standard therapy for relapsed or chemotherapy-refractory multiple myeloma patients.[6–8] Multiple myeloma is an intractable disease with poor prognosis that continues to relapse, and the duration to relapse becomes shorter in patients who repeatedly receive treatment. There are no available treatment options in which durable efficacy can be expected after relapse, and therefore effective therapeutic choices with new mechanisms of action have been long awaited.

Bortezomib is a novel small molecule that is a potent selective and reversible inhibitor of the proteasome, and has been approved for the treatment of recurrent or refractory multiple myeloma in the USA and Europe. The pharmacokinetics (PK) of bortezomib were reported in a phase I study in which it was administered in combination with gemcitabine twice weekly for 2 weeks followed by a 10-day rest period,[9] and in another phase I study in which it was administered once weekly for 4 weeks followed by a 13-day rest period.[10] Both studies were conducted in patients with advanced solid tumors and not patients with multiple myeloma. Therefore, the present phase I and II study was designed to assess the PK and pharmacodynamic (PD) effects of bortezomib in multiple myeloma patients, particularly in a Japanese population. In addition, efficacy and safety were evaluated to determine the recommended dose (RD).

Patients and Methods

Eligibility. The main eligibility criteria were: confirmed multiple myeloma according to the South-west Oncology Group diagnostic criteria;[11] had received at least previous standard front-line therapy (including melphalan and predonisone, vincristine, doxorubicin, and dexamethasone chemotherapy, and high-dose chemotherapy with autologous stem cell transplantation); had documentation of relapse or refractoriness to the last line of therapy and required therapy because of progressive disease at enrolment. Progressive disease was defined as at least one of the following: more than 25% increase in monoclonal immunoglobulin in the serum or urine; development of new osteolytic lesions or soft tissue tumors, or worsening of existing lesions; hypercalcemia (corrected serum calcium value of >11.5 mg/dL); relapse from complete response (CR); the presence of measurable disease lesions; Karnofsky performance status ≥ 60; 20–74 years of age; adequate bone marrow function (absolute neutrophil count ≥ 1000/mm^3, platelets ≥ 75 000/mm^3, and hemoglobin ≥ 8 g/dL),

[4]To whom correspondence should be addressed.
E-mail: yoshioga@is.icc.u-tokai.ac.jp

doi: 10.1111/j.1349-7006.2007.00638.x

hepatic function (aspartate aminotransferase and alanine aminotransferase levels ≤2.5 times the upper limit of institutional normal range, total bilirubin ≤1.5 times the upper limit of institutional normal range), renal function (creatinine clearance ≥ 30 mL/min), and cardiac function (left ventricular ejection fraction ≥ 55% by echocardiography without New York Heart Association class III to IV congestive heart failure) in the previous 2 weeks; and had received no systemic chemotherapy or radiotherapy in the previous 4 weeks. This study was approved by the Institutional Review Board of each participating hospital. All patients gave written informed consent and the study was conducted in accordance with Good Clinical Practice for Trials of Drugs and the Declaration of Helsinki.

Study design. The RD was determined based on the occurrence of dose-limiting toxicity (DLT) in Japanese patients and in the dose-escalating phase I of the study. The safety and efficacy of bortezomib at the RD were assessed in phase II. In phase I, three patients were enrolled in the 0.7 mg/m^2-dose group, and six patients each in the 1.0 and 1.3 mg/m^2-dose groups. DLT was defined as ≥grade 3 non-hematological toxicity or grade 4 hematological toxicity for which the relation to bortezomib could not be ruled out. The RD was defined as a dose level with a DLT incidence closest to but lower than the estimated (expected) value of 30%. Bortezomib was administered for up to six cycles.

Drug administration. Bortezomib, supplied by Janssen Pharmaceutical (Tokyo, Japan) in vials containing 3.5 mg, was administered by intravenous push over 3–5 s on days 1, 4, 8, and 11, followed by a 10-day rest period, with this 3-week period comprising one cycle. There was an interval of at least 72 h between doses.

Response and safety assessments. Patients were monitored for response after every two treatment cycles by quantitation of serum immunoglobulins, serum protein electrophoresis and immunofixation (IF), and collection of a 24-h urine specimen for total protein, electrophoresis, and IF. Response was evaluated using the European Group for Blood and Marrow Transplantation criteria,[12] after cycles 2, 4, and 6.

Adverse events were assessed and graded according to the National Cancer Institute Common Toxicity Criteria version 2.0 from the first dose until 28 days after the last dose of bortezomib.

Pharmacokinetic and pharmacodynamic analysis. Plasma bortezomib concentrations and blood 20S proteasome activity were measured in phase I. Blood samples were collected before each dose, at 5, 15, and 30 min, and 1, 2, 4, 6, 8, 12, 24, and 48 h after treatment on days 1 and 11. The measurement of plasma bortezomib concentration was conducted at Advion BioSciences (Ithaca, NY, USA) using liquid chromatography/tandem mass spectrometry (LC/MS/MS).[13] The measurement of blood 20S proteasome activity was conducted at Millennium Pharmaceuticals (Cambridge, MA, USA) using the synthetic fluorescence substrate method validated for the chymotrypsin-like activity/trypsin-like activity ratio.[14]

Results

Patients and dose escalation. The study was conducted from May 2004 to January 2006, and 34 patients were enrolled. Patient characteristics are shown in Table 1. All patients had secretory-type myeloma, and the breakdown was 20 patients (59%) with IgG type, eight patients (24%) with IgA type, three patients (9%) with light-chain type, and three patients (9%) with IgA and light-chain type. Most patients had received prior therapy with steroids, alkylating agents, and/or vinca alkaloids. Ten patients (29%) had received stem cell transplantation including high-dose therapy. The median number of lines of prior therapy was two (range: one to eight). Osteolytic lesions were observed in 30 patients (88%) and soft-tissue tumors were observed in seven (21%). The median number of treatment cycles was four (range: one to six), and the median duration of treatment was 79 days (range: 1–152 days). Ten patients (29%) completed all six cycles. The reasons for discontinuation of therapy in 25 patients were progressive disease in 11 patients, patient's own request in six patients, serious adverse events in four patients, DLT in two patients, and others in three patients. Three patients were enrolled in the 0.7 mg/m^2 group and six in the 1.0 mg/m^2 group, and no DLT were observed at any dose level. In the 1.3 mg/m^2 group, DLT (grade 3 febrile neutropenia) occurred in one of the six patients. Therefore, 1.3 mg/m^2 was determined to be the RD in subsequent phase II, in which 18 patients were enrolled.

Table 1. Patient characteristics

Patient characteristic	*n*	%
Patients	34	
Sex		
Female	12	35
Male	22	65
Age (years)		
Median	60	
Range	34–72	
Durie-Salmon stage		
I	0	
II	15	44
III	19	56
Time since diagnosis (years)		
Median	3.4	
Range	1.0–13.7	
Karnofsky performance status		
100	15	44
90–80	18	53
70–60	1	3
Serum interleukin-6 (pg/mL)		
Mean	4.2	
Range	0.5–30.2	
Cytogenetics		
Karyotype abnormal	4	12
del(13)(q14)	7	21
t(11; 14)	4	12
Prior therapy		
Chemotherapy	34	100
Steroids	34	100
Alkylating agents	33	97
Vinca alkaloids	27	79
Anthracyclines	22	65
Thalidomide	8	24
Interferon	7	21
Radiation therapy	6	18
Autologous hematopoietic stem cell transplantation	10	29

Adverse events. The safety analysis dataset consisted of all patients who received at least one dose of bortezomib (34 patients). Adverse events observed in ≥20% of patients are shown in Table 2. The events observed at a high frequency (≥50%) were lymphopenia, neutropenia, leukopenia, thrombocytopenia, anemia, asthenia, diarrhea, constipation, nausea, anorexia, and pyrexia. At least one ≥grade 3 adverse event was observed in 88% of the patients. Major ≥grade 3 adverse events were hematological toxicities including lymphopenia, neutropenia, leukopenia, thrombocytopenia, and anemia. Grade 4 hematological toxicities included neutropenia in six patients (18%), three of which experienced this adverse event during cycle 1. At least grade 3 non-hematological toxicities occurred in fewer than 10%, and no DLT during cycle 1 were observed. Grade 4 non-hematological toxicities included hematuria, blood amylase

Table 2. All adverse events occurring in at least 20% of patients ($n = 34$)

Dose (mg/m²)	0.7		1.0		1.3		All			
No. of Patients	($n = 3$)		($n = 6$)		($n = 25$)		($n = 34$)		Total	%
NCI-CTC grade	1/2	3/4	1/2	3/4	1/2	3/4	1/2	3/4		
Adverse event										
Hematologic										
Lymphopenia	3	0	4	2	8	17	15	19	34	100
Neutropenia	1	1	2	4	7	16	10	21	31	91
Leukopenia	2	0	6	0	11	12	19	12	31	91
Thrombocytopenia	1	0	4	0	12	11	17	11	28	82
Anemia	2	0	2	3	10	8	14	11	25	74
Nonhematological										
Asthenia†	3	0	3	0	15	0	21	0	21	62
Diarrhea	1	0	2	0	15	1	18	1	19	56
Constipation	2	0	3	0	14	0	19	0	19	56
Nausea	2	0	2	0	14	0	18	0	18	53
Anorexia	3	0	2	0	14	0	18	0	18	53
Pyrexia	0	0	4	0	14	0	18	0	18	53
Peripheral neuropathy‡	0	0	3	0	12	1	15	1	16	47
AST increased	1	0	1	0	11	2	13	2	15	44
LDH increased	1	0	1	0	12	1	14	1	15	44
Vomiting	1	0	0	0	9	1	10	1	11	32
Rash	0	0	1	0	10	0	11	0	11	32
ALP increased	0	0	2	0	8	0	10	0	10	29
Headache	0	0	1	0	8	0	9	0	9	27
ALT increased	1	0	1	0	7	0	9	0	9	27
Hyperglycaemia	0	0	2	0	5	0	7	0	7	21
Hyponatremia	1	0	0	1	5	0	6	1	7	21
Renal impairment	1	0	1	0	5	0	7	0	7	21
CRP increased	0	0	1	0	6	0	7	0	7	21
Weight decreased	0	0	0	0	7	0	7	0	7	21

†Including fatigue and malaise. ‡Including peripheral sensory neuropathy, peripheral motor neuropathy, and hypoesthesia. ALP, alkaline phosphatase; ALT, alanine aminotransferase; AST, aspartate aminotransferase; CRP, C-reactive protein; LDH, lactate dehydrogenase; NCI-CTC, National Cancer Institute Common Toxicity Criteria.

increase, and blood uric acid increase in one patient (3%) each. Hematuria was attributed to prostate cancer and judged as not related to bortezomib. The underlying disease was considered to be involved in the blood uric acid increase; this event was judged unlikely to be related to bortezomib. At the occurrence of grade 4 blood amylase increase, blood amylase isozymes were pancreatic-type in 86% and salivary-type in 14%. There were no gastrointestinal symptoms, such as abdominal pain, associated with amylase increase. Abdominal echography revealed no finding suggesting pancreatitis or pancreatolithiasis, and the relevant events recovered 5 days after the onset. The causality of the grade 4 blood amylase increase with bortezomib was evaluated as 'probable', and therefore treatment was continued at a reduced dose from 1.3 to 1.0 mg/m².

One case of interstitial lung disease (ILD) that resulted in a fatal outcome was observed in phase II. The patient with grade 5 ILD had developed the event on day 10 in cycle 2 after receiving seven doses of bortezomib in total. Pyrexia, non-productive cough, hypoxia, and dyspnea were observed as early symptoms, and antibiotics, antimicrobials, steroid pulse therapy, and oxygen inhalation were initiated to treat it. However, respiratory failure worsened, so the patient was put on a ventilator, and the study was discontinued. After the onset of ILD, bronchoalveolar lavage was conducted, but the causative pathogen could not be identified. The available examinations for β-D-glucan, cytomegalovirus antigenemia, influenza virus, and urinary antigen of *Legionella* were found to be negative. The diagnosis from the pathological findings was diffuse alveolar damage. A retrospective analysis of the pretreatment computed tomography (CT) images indicated that the patient had subtle interstitial shadows in the basal region of both lungs. In response, the protocol was amended to exclude patients with abnormal pretreatment bilateral interstitial shadows on CT. No cases of fatal pulmonary toxicity were observed thereafter.

Efficacy. Thirty-three patients were evaluable for efficacy, excluding one ineligible patient who had another malignancy (prostate cancer). Objective responses were observed in 10 of 33 patients (30%; 95% confidence interval 16–49%), including five IF-positive complete responses (CR^{IF+}) and five partial responses. Of the 10 responders, five patients had one line of prior therapy, two patients had three lines of prior therapy, and three patients had four or more lines of prior therapy. It is noteworthy that one patient who had received eight lines of prior therapy, including high-dose chemotherapy with autologous stem-cell transplantation, showed CR^{IF+}. Of the 10 patients who had received prior autologous hematopoietic stem cell transplantation, two patients showed CR^{IF+}, and three patients showed PR. With respect to osteolytic lesions, which is one of the efficacy endpoints, partial regression in five patients, partial disappearance in one patient, and regression of soft-tissue tumors in two patients were observed.

Pharmacokinetics and pharmacodynamics. The mean plasma bortezomib concentration–time profiles on days 1 and 11 obtained from 16 patients enrolled in phase I are shown in Fig. 1a. PK parameters obtained using non-compartmental analysis are shown in Table 3. The plasma bortezomib concentration–time

doi: 10.1111/j.1349-7006.2007.00638.x

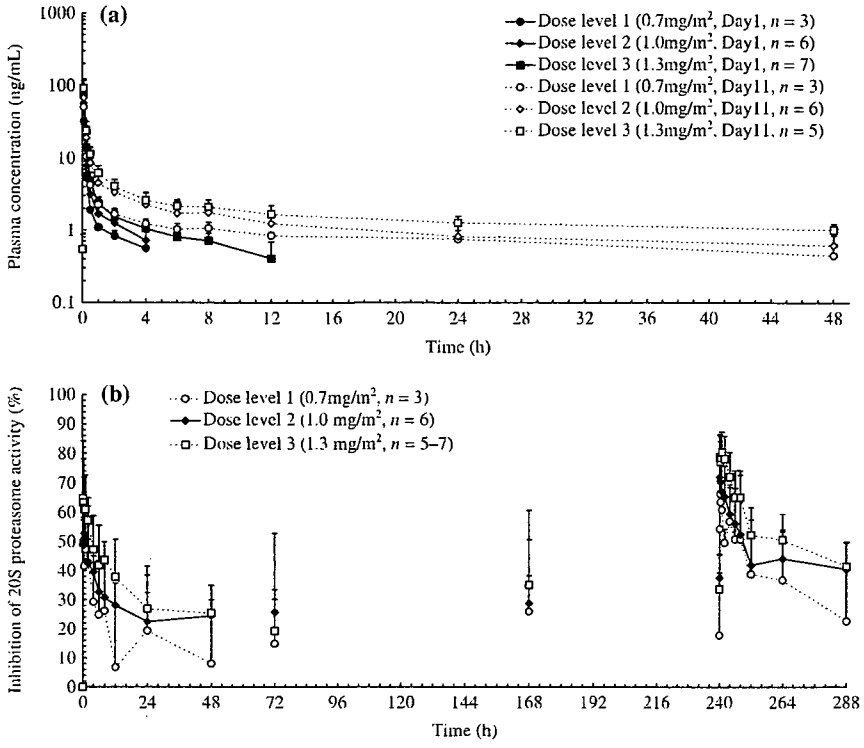

Fig. 1. (a) Plasma bortezomib concentrations (mean + SD). (b) Inhibition of blood 20S proteasome activity (mean + SD).

Table 3. Pharmacokinetic parameters (non-compartmental analysis)

Parameter	Day	Dose (mg/m²) 0.7 (n = 3)	1.0 (n = 6)	1.3 (n = 5–7)†
C_0 (ng/mL)	1	73.75 ± 7.89	144.92 ± 179.31	185.84 ± 57.65
	11	130.68 ± 71.97	147.19 ± 72.33	187.03 ± 54.31
AUC	1	14.04 ± 0.70	28.58 ± 24.86	46.50 ± 19.89
(ng · h/mL)	11	112.01 ± 47.74	108.39 ± 52.32	186.60 ± 49.79
Half life (h)	1	3.31 ± 0.88	6.81 ± 8.81	16.11 ± 20.75
	11	64.59 ± 30.29	32.46 ± 12.91	57.39 ± 24.92
Clearance	1	83.35 ± 10.52	105.41 ± 75.66	51.97 ± 18.99
(L/h)	11	11.77 ± 4.67	19.63 ± 14.50	12.10 ± 3.73
V_z (L)	1	406.92 ± 154.03	520.08 ± 349.87	894.41 ± 682.35
	11	978.51 ± 263.13	731.69 ± 242.35	957.81 ± 350.40
V_{ss} (L)	1	186.46 ± 85.02	288.90 ± 260.74	507.75 ± 558.30
	11	812.60 ± 202.03	540.03 ± 218.72	763.81 ± 271.64
C_0 ratio	11/1	1.789 ± 0.973	1.848 ± 1.133	1.103 ± 0.249
AUC ratio	11/1	7.940 ± 3.247	5.363 ± 2.970	5.142 ± 0.543

†Day 1, n = 7; day 11, n = 5. Values are mean ± SD. AUC, area under the concentration–time curve from time zero to infinity; AUC ratio, AUC on day 11/AUC on day 1; C_0, plasma concentration at the end of administration; C_0 ratio, C_0 on day 11/C_0 on day 1; V_z, the apparent volume of distribution during the terminal phase; V_{ss}, the apparent volume of distribution at steady state.

profiles showed a biphasic elimination profile, characterized by rapid distribution followed by a longer elimination at all dose levels. At any dose level, the elimination half-life ($t_{1/2}$) on day 11 was prolonged, and systemic clearance (CL) was lower compared with day 1. Therefore, delayed elimination of bortezomib from plasma associated with repeated administrations was observed, and the plasma bortezomib concentration after administration (C_0, estimated value) and area under the plasma concentration–time curve (AUC) showed higher values on day 11 compared with day 1. AUC showed dose dependency, whereas C_0 did not.

The inhibition of blood 20S proteasome activity is shown in Fig. 1b. The 20S proteasome inhibition recovered over time at all dose levels, but was prolonged compared with the temporal decrease in plasma bortezomib concentration, and the inhibition was still observed before treatment on days 4, 8, and 11.

Discussion

In the present study, bortezomib was generally well tolerated in the 25 Japanese patients whose treatments were started at the RD of 1.3 mg/m². Hematological toxicities, gastrointestinal toxicities, and peripheral neuropathies observed in our patients were similar to those reported for patients in clinical studies from the USA and Europe.[15,16] Most could be managed without interventions or with the usual symptomatic therapy. Grade 4 neutropenia was observed in 18% of patients, but treatment could be continued with dose reduction. The response rate obtained in the present study was comparable to that reported by Richardson *et al.* in a pivotal phase III study.[16] In addition, patients who had received heavy prior therapy also showed a consistent response. Therefore, 1.3 mg/m² is considered appropriate as an initial dose of bortezomib in Japanese patients. There was a fatal pulmonary disorder event (ILD) in one patient treated with the 1.3 mg/m² dose in which a causal relationship with bortezomib could not be ruled out. Hence, special care should be taken prior to initiating treatment with bortezomib to evaluate patients (e.g. chest X-ray or chest CT scan) and during and after bortezomib treatment if they develop subjective symptoms such as dyspnea, cough, and fever.

The assessment of PK and PD in multiple myeloma patients treated with bortezomib twice weekly for 2 weeks was conducted for the first time in Japanese patients. A decrease in CL associated with increased exposures and subsequently longer $t_{1/2}$ values were observed after repeated administration and dose escalation. The relatively large volume of distribution suggests that bortezomib may be distributed extensively into the extravascular tissues. It can be postulated that CL values on day 1 are apparent values observed due to rapid tissue distribution, whereas

saturation of proteasome binding sites and tissue distribution occur after multiple dosing, and the CL value on day 11 may be a better representation of the true value.

It was also found that the blood 20S proteasome inhibition at each dose level recovered over time, but was prolonged compared with the temporal decrease in plasma bortezomib concentration. Similarly to CL, this could be due to the large distribution volume of bortezomib and its slow return from tissues to plasma.

Delayed elimination and enhanced proteasome inhibition were observed with repeated administration and dose increase, but no clear tendency in the incidence or degree of adverse reactions was observed. However, the PD results of the present study in Japanese patients demonstrate that the inhibition of 20S proteasome activity does not recover even after 72 h, which is specified as a minimum interval for bortezomib dosing. Accordingly, when bortezomib is used in clinical practice, it is important to determine the optimal dosage and determine whether it is appropriate to administer bortezomib while considering the balance between safety and efficacy.

Acknowledgments

We thank all of the investigators, physicians, nurses, and clinical research coordinators at Tokai University School of Medicine, National Cancer Center Hospital, Aichi Cancer Center, and National Cancer Center Hospital East. We give recognition to Dr A. Togawa (Kofu National Hospital, Kofu, Japan), Dr Y. Sasaki (Saitama Medical University, Saitama, Japan), and Dr K. Hatake (Cancer Institute Hospital, Japanese Foundation for Cancer Research, Tokyo, Japan) for their strict review of the clinical data as members of the Independent Data Monitoring Committee.

References

1 Oken MM. Standard treatment of multiple myeloma. *Mayo Clin Proc* 1994; **69**: 781–6.
2 Oken MM. Management of myeloma: current and future approaches. *Cancer Control* 1998; **5**: 218–25.
3 Paccagnella A, Chiarion-Sileni V, Soesan M *et al.* Second and third responses to the same induction regimen in relapsing patients with multiple myeloma. *Cancer* 1991; **68**: 975–80.
4 Attal M, Harousseau J, Stoppa J *et al.* A prospective, randomized trial of autologous bone marrow transplantation and chemotherapy in multiple myeloma. *N Eng J Med* 1996; **335**: 91–7.
5 Child JA, Morgan GJ, Davies FE *et al.* High-dose chemotherapy with hematopoietic stem-cell rescue for multiple myeloma. *N Engl J Med* 2003; **348**: 1875–83.
6 Barlogie B, Smith L, Alexanian R. Effective treatment of advanced multiple myeloma refractory to alkylating agents. *N Engl J Med* 1984; **310**: 1353–6.
7 Alexanian R, Barlogie B, Dixon D. High-dose glucocorticoid treatment of resistant myeloma. *Ann Intern Med* 1986; **105**: 8–11.
8 Buzaid AC, Durie BG. Management of refractory myeloma: a review. *J Clin Oncol* 1988; **6**: 889–905.
9 Appleman LJ, Ryan DP, Clark JW *et al.* Phase 1 dose escalation study of bortezomib and gemcitabine safety and tolerability in patients with advanced solid tumors. *39th Annual Meeting of the American Society of Clinical Oncology* 2003 (abstract 839).
10 Papandreou CN, Daliani DD, Nix D *et al.* Phase I trial of the proteasome inhibitor bortezomib in patients with advanced solid tumors with observations in androgen-independent prostate cancer. *J Clin Oncol* 2004; **22**: 2108–21.
11 Huang Y, Hamilton A, Arnuk OJ, Chaftari P, Chemaly R. Current drug therapy for multiple myeloma. *Drugs* 1999; **57**: 485–506.
12 Blade J, Samson D, Reece D *et al.* Criteria for evaluating disease response and progression in patients with multiple myeloma treated by high-dose therapy and haemopoietic stem cell transplantation. Myeloma Subcommittee of the EBMT. *European Group for Blood Marrow Transplant Br J Haematol* 1998; **102**: 1115–23.
13 Nix DJ, Pien C, LaButti J *et al.* Clinical pharmacology of the proteasome inhibitor PS-341. *AACR-NCI-EORTC International Conference on Molecular Targets and Cancer Therapeutics* 2001 (abstract 389).
14 Lightcap ES, McCormack TA, Pien CS *et al.* Proteasome inhibition measurements: clinical application. *Clin Chem* 2000; **46**: 673–83.
15 Richardson PG, Barlogie B, Berenson J *et al.* A phase 2 study of bortezomib in relapsed, refractory myeloma. *N Engl J Med* 2003; **348**: 2609–17.
16 Richardson PG, Sonneveld P, Schuster MW *et al.* Bortezomib or high-dose dexamethasone for relapsed multiple myeloma. *N Engl J Med* 2005; **352**: 2487–98.

doi: 10.1111/j.1349-7006.2007.00638.x

British Journal of Cancer (2007) 97, 778–784

www.bjcancer.com

Evaluation of epidermal growth factor receptor mutation status in serum DNA as a predictor of response to gefitinib (IRESSA)

H Kimura*[,1], M Suminoe[2], K Kasahara[1], T Sone[1], T Araya[1], S Tamori[1], F Koizumi[3], K Nishio[3,4], K Miyamoto[2,5], M Fujimura[1] and S Nakao[1]

[1]*Department of Respiratory Medicine, Kanazawa University Hospital, Takara-machi 13-1, Kanazawa, Ishikawa 920-8641, Japan;* [2]*Department of Clinical Pharmacy, Graduate School of Natural Science and Technology, Kanazawa University, Takara-machi 13-1, Kanazawa, Ishikawa 920-8641, Japan;* [3]*Shien-Lab, National Cancer Center Hospital, Tsukiji 5-1, Chuo-ku, Tokyo 104-0045, Japan;* [4]*Department of Genome Biology, Kinki University School of Medicine, 377-2 Ohno-Higashi Osaka-Sayama, Osaka 589-8511, Japan;* [5]*Department of Hospital Pharmacy, School of Medicine, Kanazawa University, Takara-machi 13-1, Kanazawa, Ishikawa 920-8641, Japan*

The aim of this study was to evaluate the usefulness of *EGFR* mutation status in serum DNA as a means of predicting a benefit from gefitinib (IRESSA) therapy in Japanese patients with non-small cell lung cancer (NSCLC). We obtained pairs of tumour and serum samples from 42 patients treated with gefitinib. *EGFR* mutation status was determined by a direct sequencing method and by Scorpion Amplification Refractory Mutation System (ARMS) technology. *EGFR* mutations were detected in the tumour samples of eight patients and in the serum samples of seven patients. *EGFR* mutation status in the tumours and serum samples was consistent in 39 (92.9%) of the 42 pairs. *EGFR* mutations were strong correlations between both *EGFR* mutation status in the tumour samples and serum samples and objective response to gefitinib ($P<0.001$). Median progression-free survival time was significantly longer in the patients with *EGFR* mutations than in the patients without *EGFR* mutations (194 *vs* 55 days, $P=0.016$, in tumour samples; 174 *vs* 58 days, $P=0.044$, in serum samples). The results suggest that it is feasible to use serum DNA to detect *EGFR* mutation, and that it's potential as a predictor of response to, and survival on gefitinib is worthy of further evaluation.
British Journal of Cancer (2007) **97,** 778–784. doi:10.1038/sj.bjc.6603949 www.bjcancer.com
Published online 11 September 2007

Keywords: EGFR; mutation; serum; gefitinib

Lung cancer is a major cause of cancer-related mortality worldwide and is expected to remain a major health problem for the foreseeable future (Parkin *et al*, 2005). Most patients have advanced disease at the time of diagnosis. Initial therapy for advanced non-small cell lung cancer (NSCLC) is typically systemic chemotherapy with a two-drug combination regimen, which often includes a platinum agent, but the median survival of patients treated with such regimens has ranged from only 8 to 10 months (Breathnach *et al*, 2001; Kelly *et al*, 2001; Schiller *et al*, 2002). Little improvement in the efficacy of chemotherapy has been made in the last 20 years. A recent report shows that the addition of bevacizumab, a monoclonal antibody against vascular endothelial growth factor, to paclitaxel plus carboplatin in patients with advanced NSCLC has a significant survival benefit, and the median survival was 12.3 months, as compared with 10.3 months in the chemotherapy-alone group (Sandler *et al*, 2006).

Targeting epidermal growth factor receptor (EGFR) is an appealing strategy for the treatment of NSCLC, because EGFR has been found to be expressed, sometimes strongly, in NSCLC (Franklin *et al*, 2002). Gefitinib ('Iressa', AstraZeneca) is a small molecule and selective EGFR tyrosine kinase inhibitor (EGFR-TKI) that has shown antitumour activity in NSCLC patients as a single agent in phase II and III trials (Fukuoka *et al*, 2003; Thatcher *et al*, 2005). An association between mutations in *EGFR* tyrosine kinase sites in NSCLC patients and hyper-responsiveness to gefitinib has recently been reported (Lynch *et al*, 2004; Paez *et al*, 2004). The mutations consisted of small in-frame deletions or substitutions clustered around the ATP-binding site in exons 18–21 of *EGFR*. Some investigators subsequently found that *EGFR* mutations are one of the strong determinants of tumour response to EGFR tyrosine kinase inhibitors (Pao *et al*, 2004; Han *et al*, 2005; Shigematsu *et al*, 2005). The mutation status could be evaluated stably in studies that used surgical tissues to detect the *EGFR* mutations, but most patients who require gefitinib therapy already have advanced disease at the time of diagnosis and therefore are not operated on. It is difficult to obtain sufficient tumour DNA from non-surgical tissue samples, for example, those derived from bronchoscopy that allow detection of *EGFR* mutations by direct sequencing. Actually, translational research in patients with advanced NSCLC in whom gefitinib therapy recommended has been limited by the scarcity of available tumour biopsy tissue, and tumour samples for genetic research were only available for 12.7 and 44.5%, respectively, of patients enrolled in two large phase III clinical studies with EGFR-TKIs (Tsao *et al*, 2005; Hirsch *et al*, 2006). It is therefore important to have sensitive methods for detecting *EGFR* mutations from DNA derived from non-surgical tissue specimens.

*Correspondence: Dr H Kimura;
E-mail: kimura@med3.m.kanazawa-u.ac.jp
Received 2 July 2007; accepted 30 July 2007; published online 11 September 2007

It is well known that the concentration of circulating DNA in plasma or serum has been found to be higher in cancer patients than in cancer-free control subjects, and that significantly higher DNA levels are found in the serum of patients with metastatic disease (Leon *et al*, 1977; Jahr *et al*, 2001; Sozzi *et al*, 2003). The tumour-derived DNA in serum may have been released by a tumour mass that has undergone cell necrosis or tumour cells lysis, or by circulating tumour cells, resulting in a very elevated serum DNA concentration. Some investigators have shown that testing for DNA alterations in peripheral blood has great potential, especially for early detection and diagnosis and for monitoring for a relapse during follow-up (Chen *et al*, 1996; Nawroz *et al*, 1996; Sozzi *et al*, 1999, 2001; Cuda *et al*, 2000; Nunes *et al*, 2001). The same alterations which mean mutations, methylation, and loss of heterozygosity, in genomic DNA have been observed in DNA from both tumour cells in resected and biopsy specimens, and from serum samples in patients with various types of tumours, including NSCLC (Sanchez-Cespedes *et al*, 1998; Esteller *et al*, 1999). Some studies have even reported that genetic aberrations in serum DNA modulate survival in NSCLC patients treated with chemotherapy. Their authors have proposed that the assay used in their studies may obviate the need for tumour tissue analysis (Ramirez *et al*, 2005; de las Penas *et al*, 2006). Serum samples can be obtained safely, with the option of repeat sampling from all NSCLC patients regardless of patient characteristics. The detection of *EGFR* mutations in serum provides a unique and potentially valuable tumour marker for prediction of response and prognosis.

We have previously reported the feasibility of detecting *EGFR* mutations in serum DNA using the Scorpion Amplification Refractory Mutation System (ARMS) method (Kimura *et al*, 2006). The Scorpion ARMS method is one of the most sensitive and fastest methods for specific detection of mutations in DNA (Newton *et al*, 1989; Whitcombe *et al*, 1999). Although *EGFR* mutations were detectable by both PCR direct sequencing, which has generally been used to detect the mutations and the Scorpion ARMS method, mutation status determined with Scorpion ARMS predicted response to gefitinib in our study (Kimura *et al*, 2006). Since the previous study did not clarify the feasibility of using serum DNA as a practical source for detection of *EGFR* mutations, in the present study, we sought to demonstrate that *EGFR* mutation status determined in serum DNA is the same as in actual tumour samples.

The aim of this study was (1) to determine whether the *EGFR* mutations in tumour tissue and serum samples from advanced NSCLC patients are the same, and (2) to identify whether there is a correlation between *EGFR* mutation status detected in serum DNA and both response to gefitinib and survival benefit from gefitinib.

PATIENTS AND METHODS

Patients

The subjects were patients with advanced NSCLC in whom gefitinib therapy was started between July 2002 and February 2006. All patients were treated with gefitinib alone, and 14 patients were treated with gefitinib as initial therapy. The others were treated with gefitinib as second- or third-line therapy. The diagnosis of NSCLC was based on the histological or cytological findings, and the histological type was determined according to WHO criteria (Travis *et al*, 1999). Patients' records consisted of age, gender, smoking habit, and histological tumour type. Patients were divided into three groups according to their smoking status: never-smokers (<100 cigarettes per lifetime), former smokers ($\geqslant 100$ cigarettes per lifetime, but quit 1 year before diagnosis), and current smokers ($\geqslant 100$ cigarettes per lifetime). The response to gefitinib was evaluated in accordance with the 'Response Evaluation Criteria in Solid Tumours (RECIST)' guidelines (Therasse *et al*, 2000). This study was approved by the Institutional Review Board of Kanazawa University Hospital. Written informed consent was obtained from all participants. No research results were entered into the patient's records or released to the patient or the patient's physician.

Tissue preparation and DNA extraction

Tumour specimens were obtained at diagnosis and analysed retrospectively. Twenty-eight tumour samples were collected from the primary cancer (19 via transbronchial lung biopsy, 2 via percutaneous lung biopsy, and 7 surgical specimens). Fourteen tumour samples were from metastatic sites (three from bone, eight lymph nodes, one brain, and one small bowel). All specimens were examined histologically to confirm the diagnosis of NSCLC. The tumour specimens obtained were fixed in formalin and embedded in paraffin wax. Serial sections containing representative malignant cells were deparaffinised in xylene washes and dehydrated in 100% ethanol. DNA was extracted from five serial 10-μm thick sections by using the QIAamp DNA Mini kit (Qiagen, Hilden, Germany) according to the protocol described in the manufacturer's instructions. The DNA obtained was eluted in 50 μl of buffer AE, and the concentration and purity of the extracted DNA were assessed by spectrophotometry. The extracted DNA was stored at -20°C until used.

Blood sample collection and DNA extraction

Blood samples were collected before the start of gefitinib therapy. The volume of each blood sample was 4 ml. Serum was separated within 2 h from the sample collection and stored at -80°C until used. Serum DNA was extracted and purified by using a Qiamp Blood Kit (Qiagen), with the following protocol modifications. One column was used repeatedly until the whole sample had been processed. The resulting DNA was eluted in 50 μl of sterile bi-distilled buffer. The concentration and purity of the extracted DNA were determined by spectrophotometry. The extracted DNA was stored at -20°C until used.

Direct sequencing for detection of *EGFR* mutations

EGFR mutations in exons 18, 19, and 21 were detected by PCR-based direct sequencing. PCR amplification was performed in 10 ng of genomic DNA using the TaKaRa Ex Taq™ Hot Start Version kit (TaKaRa, Tokyo, Japan). The primers (forward and reverse) were: exon 18 (5′-CCTTGTCTCTGTGTTCTTGT-3′ and 5′-CTGCGGCCCAGCCCAGAGGC-3′), exon 19 (5′-CATGTGGCAC CATCTCACA-3′ and 5′-CCACACAGCAAAGCAGAA AC-3′), and exon 21 (5′-CAGGGTCTTCTCTGTTTCAG-3′ and 5′-TAAAGC CACCTCCTTACTTT-3′). DNA was amplified for 35 cycles at 95°C for 30 s, 61°C for 30 s, and 72°C for 60 s followed by 7 min of extension at 72°C. Sequencing was performed with a 3100 Genetic Analyzer (Applied Biosystems, Foster City, CA, USA), and the results were analysed with Sequencer 3.11 software (Applied Biosystems) to compare variations. The sequences were compared with the GenBank human sequence for *EGFR* (accession number AF288738).

Scorpion ARMS for detection of E746_A750del and L858R

An EGFR Scorpion Kit (DxS Ltd, Manchester, UK), which combines two technologies, namely ARMS and Scorpion was to detect mutations in real-time PCR as described previously (Kimura *et al*, 2006). Four scorpion primers for detection of E746_A750del, L858R, and the wild type in both exons 19 and 21 were designed and synthesised by DxS Ltd. All reactions were performed in 25 μl volumes using 1 μl of template DNA, 7.5 μl of reaction buffer mix, 0.6 μl of Primer mix and 0.1 μl of Taq polymerase. All reagents are

included in the kit. Real-time PCR was carried out by using SmartCycler® II (Cepheid, Sunnyvale, CA, USA) under the following conditions: initial denaturation at 95°C for 10 min, 50 cycles of 95°C for 30 s, 62°C for 60 s with fluorescence reading (set to FAM, which allows optical excitation at 480 nm and measurement at 520 nm) at the end of each cycle. Data analysis was performed with Cepheid SmartCycler software (version 1.2b). The cycle threshold (C_t) was defined as the cycle at the highest peak of the second-derivative curve, which represented the point of maximum curvature of the growth curve. Both C_t and maximum fluorescence (F_l) were used to interpret the results. Positive results were defined as follows: $C_t \leqslant 45$ and $F_l \geqslant 50$. These analyses were performed in duplicate for each sample and reviewed by two investigators blinded to any clinical information.

Statistical analyses

Patient characteristics, including gender, tumour histology, smoking habit, and response to gefitinib, were tabulated according to mutation status. Fisher's exact test was used to test for associations between the presence of *EGFR* mutations and the patients' characteristics. Overall survival (OS) and progression-free survival (PFS) according to *EGFR* mutation status were estimated by the Kaplan–Meier method, and compared using the two-sided log-rank test. Overall survival was defined as the interval between the start of gefitinib therapy and death from any cause; patients known to be still alive at the time of the analysis were censored at the time of their last follow-up. Progression-free survival was defined as the interval between the start of gefitinib therapy and the first manifestation of progressive disease (PD) or death from any cause; patients known to be alive and without PD at the time of analysis were censored at the time of their last follow-up.

RESULTS

Patient's characteristics

Forty-two patients were enrolled in this study (Table 1). This study covered a long period. There are two reasons why it took 4 years to assemble the 42 patients enrolled. One is that this study was carried out in Kanazawa University Hospital alone, and was not a multicentre study. The other is that not all patients with NSCLC at the hospital during that period were enrolled in this study, because some were enrolled in other trials or the patients refused. Their median age was 58 years (range, 40–81 years), and there were 14 females (33.3%) and 14 never-smokers (33.3%). The histological and/or cytological diagnosis was adenocarcinoma in 31 patients (73.8%), squamous cell carcinoma in 7 (16.7%), and large-cell carcinoma in 4 (9.5%). The results for response to gefitinib showed that 10 patients (23.8%) had a partial response (PR) and 14 (33.3%) had stable disease (SD). The other 18 patients (42.9%) had PD. Serum DNA was extracted in all 42 samples at a median concentration of 62.0 ng ml^{-1} (range, 0–342.8). The concentrations in 10 samples were below the minimum concentration detectable.

Table 1 Patient characteristics and *EGFR* mutation status

	(n)
No. of patients	42
Age (years)	
Median	58
Range	40–1
Gender	
Male	28 (66.7%)
Female	14 (33.3%)
Smoking habit	
Current	20 (47.6%)
Former	8 (19.1%)
Never	14 (33.3%)
Histology	
Adenocarcinoma	31 (73.8%)
Squamous cell carcinoma	7 (16.7%)
Large-cell carcinoma	4 (9.5%)
Response to gefitinib	
Partial response	10 (23.8%)
Stable disease	14 (33.3%)
Progressive disease	18 (42.9%)

EGFR mutation status detected

Direct sequencing of PCR products from tumour tissues of all patients allowed their mutation status to be determined. Both direct sequencing and Scorpion ARMS allowed mutation status to be determined in the serum samples of all patients. As summarised in Table 2, mutations were identified in 9 (21.4%) of the 42 patients. Mutations in eight patients were detected in tumour samples and seven in serum samples. Five mutations were deletion mutations located in exon 19 (E746_A750del in four and L747_T751del in one). Four mutations were substitution mutations located in exon 21 (L858R), and one was a substitution mutation located in exon 18 (V689L). One patient had double substitution mutations (V689L and L858R). The E746_A750 deletion and L858R substitution mutation were the most common (8 out of 9, 88.9%), and both are well-known hot spot mutations described previously (Kosaka *et al*, 2004; Han *et al*, 2005). There were no T790M mutations identified by direct sequencing on tumour samples or serum samples. Of the nine patients with mutations, six (66.7%) were never-smokers, and five (55.6%) were female patients. Almost all of the patients with mutations had adenocarcinoma (8 out of 9, 88.9%).

Sensitivity and specificity of detection in serum DNA

In six of the patients, the same *EGFR* mutation was detected in both the tumour sample and the serum sample. There were no *EGFR* mutations detected in either the tumour sample or serum sample from 33 of the patients. *EGFR* mutation status was consistent in 39 (92.9%) of the 42 of the pairs (Table 3). In two patients the tumour samples was positive for an *EGFR* mutation and the serum sample was negative. The concentrations of serum DNA in the two patients were below the minimum level of detection by spectrophotometry. In one patient, the serum sample was positive for an *EGFR* mutation and the tumour sample was negative. The tumour sample that contained no mutations from the patient whose serum was positive for a mutation was collected by transbronchial lung biopsy.

Correlation between *EGFR* mutation status and patient characteristics

Detection of *EGFR* mutations occurred significantly more frequently in the serum DNA from the never-smokers (never-smokers 5 out of 14 (35.7%); current/former smokers 2 out of 28 (7.1%); $P = 0.031$) (Table 4). Mutations were more frequently detected in the DNA from tumour samples of never-smokers than of current/former smokers (never-smokers 5 out of 14 (35.7%); current/former smokers 3 out of 28 (10.7%); $P = 0.092$), but the difference was not statistically significant. Mutations were detected more frequently in the samples from females (tumour: females 5 out of 14 (35.7%), males 3 out of 28 (10.7%); serum: females 3 out

Table 2 Patients with *EGFR* mutation

Age	Gender	Histology	Stage	Smoking	Response	EGFR mutation status: Tumour tissue	EGFR mutation status: Serum
44	M	Ad	Re	Never	PR	E746_A750del	E746_A750del
79	M	Ad	IV	Former	PR	L858R	L858R
53	M	Ad	IV	Never	PR		V689L, L858R*
59	M	La	IV	Current	PD	E746_A750del	E746_A750del
63	F	Ad	IIIB	Never	PR	L858R	
62	F	Ad	IV	Never	PR	E746_A750del	E746_A750del
56	F	Ad	IV	Never	PR	E746_A750del	E746_A750del
57	F	Ad	IIIB	Former	SD	E746_T751del	
62	F	Ad	IV	Never	PR	L858R	L858R

Ad = adenocarcinoma; del = deletion; EGFR = epidermal growth factor receptor; F = female; La = large-cell carcinoma; M = male; PD = progressive disease; PR = partial response; Re = recurrence after surgery; SD = stable disease. The numbering of the mutation sites was based on NP_005219.2 (amino acid). *L858R was detected both by Scorpion ARMS and direct sequencing. V689L was detected by direct sequencing. All samples detected in serum DNA but the samples (*) were detected by Scorpion ARMS alone.

Table 3 Sensitivity for detection of *EGFR* mutations in serum samples

		Serum: +	Serum: −
Tumour tissue	+	6	2
	−	1	33

EGFR = epidermal growth factor receptor; + = mutation positive; − = mutation negative.

Table 4 Frequency of *EGFR* mutations

	Tumour tissue +	Tumour tissue −		Serum +	Serum −	
(A) Gender and EGFR mutation status						
Female	5	9		3	11	
Male	3	25	$P=0.092$	4	24	$P=0.669$
(B) Histology and EGFR mutation status						
Ad	7	24		6	25	
Non-Ad	1	10	$P=0.657$	1	10	$P=0.654$
(C) Smoking habit and EGFR mutation status						
Never	5	9		5	9	
Current/former	3	25	$P=0.092$	2	26	$P=0.031$
(D) Response to gefitinib						
PR	6	4		6	4	
SD/PD	2	30	$P<0.001$	1	31	$P<0.001$

Ad = adenocarcinoma; EGFR = epidermal growth factor receptor; PD = progressive disease; PR = partial response; SD = stable disease; + = mutation positive; − = mutation negative. *P*-value: Fisher's exact test.

of 14 (27.2%), males 4 out of 28 (14.3%)) and from patients with adenocarcinoma (tumour: adenocarcinoma 7 out of 31 (22.6%), non-adenocarcinoma 1 out of 11 (9.1%); serum: adenocarcinoma 6 out of 31 (19.4%), non-adenocarcinoma 1 out of 11 (9.1%)), but the differences were not statistically significant. There were no statistically significant differences in demographic characteristics between the patients with *EGFR* deletion mutations and patients with *EGFR* substitution mutations (data not shown).

Correlation between *EGFR* mutation status and response to gefitinib

EGFR mutations were detected significantly more frequently in responders to gefitinib. Seven of the nine patients with mutations had a PR to gefitinib. Comparison between *EGFR* mutation status and response to gefitinib showed that *EGFR* mutation was more frequent in patients with a PR than in patients with SD/PD (Table 4D).

EGFR mutations are associated with increased survival

The median PFS and OS of the patients treated with gefitinib was 60 days (95% CI, 52–68) and 228 days (95% CI, 150–306), respectively. Patients with *EGFR* mutations in both tumour samples and serum samples had a significantly longer median PFS than the patients without *EGFR* mutations (194 *vs* 55 days, $P=0.016$, in tumour samples; 174 *vs* 58 days, $P=0.044$, in serum samples; Figure 1A). The patients with *EGFR* mutations had a longer median OS than the patients without *EGFR* mutations, but the difference was not statistically significant (716 *vs* 193 days, $P=0.070$, in tumour samples; 387 *vs* 228 days, $P=0.489$, in serum samples; Figure 1B). These results suggest that the patients who were serum *EGFR*-mutation-positive had better outcomes of gefitinib therapy in terms of PFS, OS, and response, than patients who were *EGFR*-mutation-negative. In addition smoking status (never-smoker *vs* former/current smoker) was found to be an independent predictor of longer PFS ($P=0.002$) and longer OS ($P=0.035$). Progression-free survival and OS were longer in female patients and patients with adenocarcinoma than in male patients and non-adenocarcinoma patients, respectively, but the differences were not statistically significant.

DISCUSSION

We previously reported detecting *EGFR* mutations in serum DNA by Scorpion ARMS method and that mutation status is useful for predicting response to gefitinib (Kimura *et al*, 2006). The two major findings in the present study provide additional support for the use of serum DNA as an alternative to tumour samples for detection of *EGFR* mutations in patients with advanced NSCLC. First, these results demonstrate that *EGFR* mutation status in serum DNA was the same as in tumour samples in almost every patient. In addition, mutation status in serum DNA predicted for a significantly greater response and time to progression with gefitinib, as well as showing a trend towards increased OS in patients treated with gefitinib. The results confirm the clinical